1 Introduction

This thesis presents the results of a research program aimed at identifying the major controls of the porphyry-related Kucing Liar Cu-Au mineralised system. Porphyry-related mineralisation provided over 50% of the world's Cu production in the 20th century (Hedenquist and Richards, 1998) and these types of deposits are among the largest reservoirs of gold in the upper crust (Kesler, *et al.*, 2002). Economic Cu ± Mo ± Au deposits associated with porphyry magmas are concentrated at the margins of the Pacific Rim, occurring in North and South America, while in the southwest Pacific they are concentrated in Philippines, New Guinea and Indonesia (Figure 1-1). Due to the economic importance of porphyry mineralisation there is a large body of literature concerning this class of deposit. There is a wide variety of mineralisation styles associated with porphyritic intrusions including porphyry, skarn, epithermal and mantos that are enriched to varying degrees with Mo, Cu, Au, Ag, Pb and Zn (Figure 1-2).

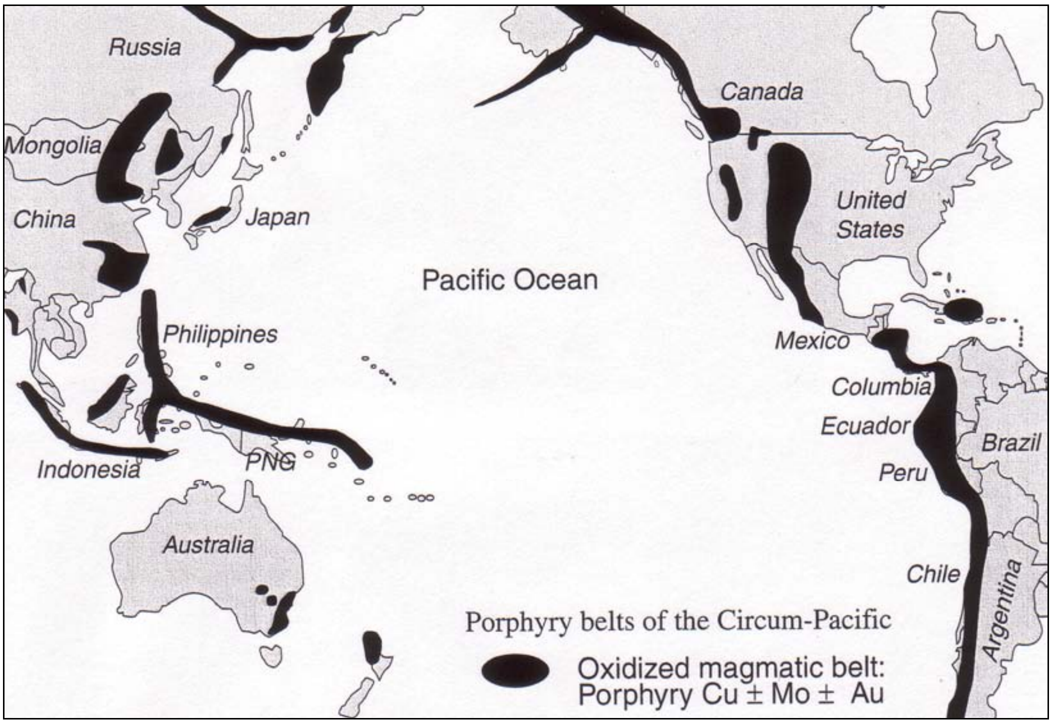

Figure 1-1 Distribution of porphyry Cu±Mo±Au deposits in the circum-Pacific region
Reproduced from Tosdal and Richards (2001)

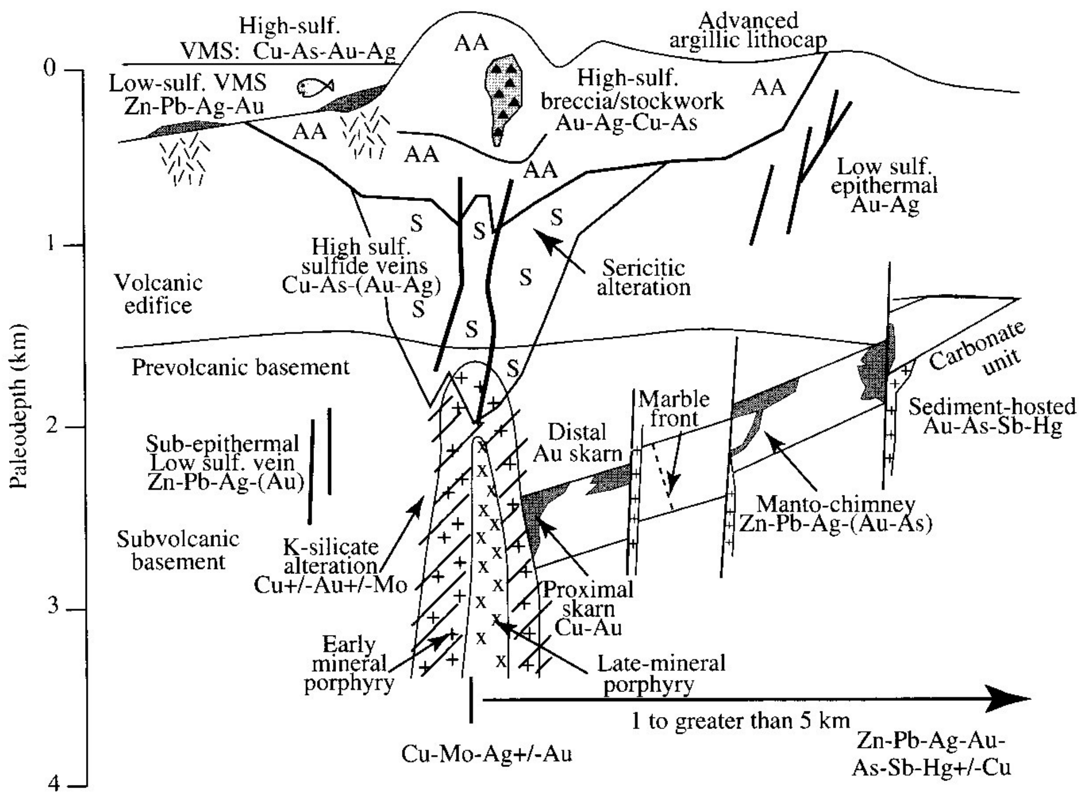

Figure 1-2 Ore deposit environments related to porphyritic intrusions

Schematic diagram showing the various forms of alteration associated with porphyry-related hydrothermal systems (figure 2 of Tosdal and Richards, 2001).

Kucing Liar is a Cu-Au mineralised system forming part of the Ertsberg Mining District, which is situated in the easternmost Indonesian province of Irian Jaya, now increasingly referred to as West Papua (Figure 1-3). PT Freeport Indonesia has been operating in the Ertsberg Mining District since 1967. Irian Jaya is part of the tectonic entity of New Guinea which includes a number of islands to the east which make up the Melanesian Volcanic Arc (Figure 1-4). New Guinea itself is dominated by a mountain range that extends the length of the island, commonly reaching elevations above 4,000m, referred to as the Papuan Fold Belt, which has a characteristic sigmoid shape from east to west and is noticeably wider in the middle of the island in the vicinity of the Papua New Guinea Highlands.

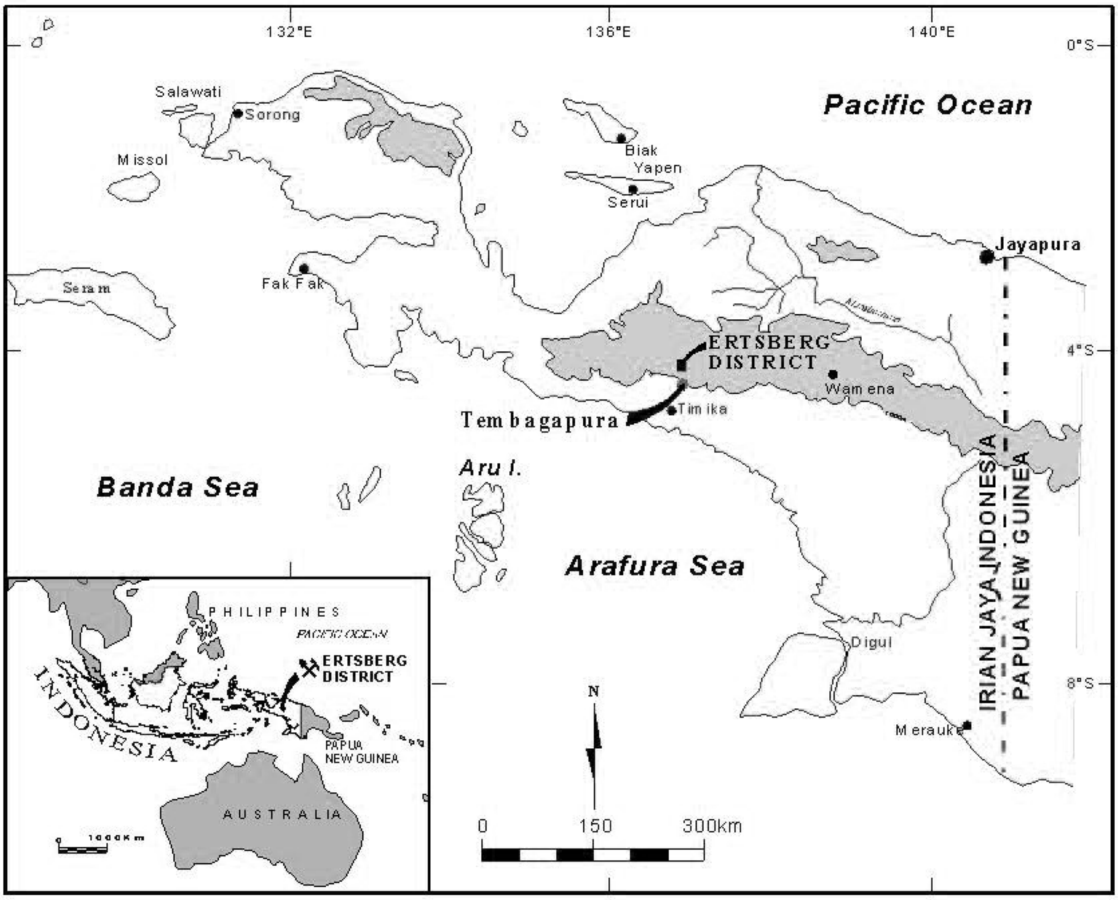

Figure 1-3 Location of the Ertsberg Mining District

Shaded area of map indicates areas above 1,000m elevation. Figure supplied by PT Freeport Indonesia.

The Ertsberg Mining District possesses the world's largest currently exploited gold resource and third largest copper resource, with the largest contribution being the Grasberg deposit. The Grasberg copper budget is of similar scale to the giant porphyry deposits of the southwest USA and Chile (Cooke *et al.*, 2005). The well-studied Bingham Canyon deposit in Utah has a similar copper inventory to Grasberg but significantly lower gold content. The deposits associated with the New Guinea tectonic system host the largest amount of copper and gold in the western Pacific (Garwin *et al.*, 2005). Papua New Guinea contains a large number of gold ± copper deposits that are notably more gold-dominant than the Ertsberg mining district. At the time of data collection for this research (1998-2000), the Kucing Liar system was estimated to include 321Mt or ore containing 1.41% Cu and 1.41g/t Au. However, continued resource definition drilling has confirmed a larger resource of 478Mt of ore containing 1.29%Cu and 1.14g/tAu at Kucing Liar

(PT Freeport Indonesia, 2002 annual report). Within the district, nine major copper and/or gold occurrences have been delineated (Table 1-1), including gold-only resources (Wanagon) as well as copper-only resources (Lembah Tembaga) as well as other resources with variable grades and Cu:Au ratios. While Kucing Liar is much smaller than Grasberg, at ~540t of contained gold, it rates in the top 10 gold deposits of the world. The high copper *and* gold grades in such large quantities as well as the relationship to a richly gold-endowed island arc makes Grasberg and its related deposits unique amongst world-class porphyry copper deposits and so of particular interest in understanding their genesis. The different deposits found in the district display distinct and unique characteristics. Macdonald and Arnold (1994), Hefton *et al.*, (1995), and Pollard and Taylor (2002) have described the geology, alteration and mineralisation of the Grasberg Igneous Complex, while Mertig et al. (1994), Meinert et al. (1997) and Prendergast et al. (2005) have described the occurrences of sedimentary-hosted mineralisation in the district.

Table 1-1 Copper and/or gold resources of the Ertsberg Mining District

Deposit	Ore (t)	Cu (%)	Au (g/t)	Copper (t)	Gold (oz)
Grasberg	2,150,000,000	1.14	1.19	24,510,000	82,258,946
Kucing Liar	478,000,000	1.29	1.14	5,449,200	17,519,583
Ertsberg East Skarn System	185,000,000	1.58	0.71	2,923,000	4,223,065
Lembah Tembaga	90,000,000	1.50	na	1,350,000	Na
Big Gossan	37,349,000	2.69	1.02	1,004,688	1,224,833
Ertsberg	32,600,000	2.30	0.80	749,800	838,504
Dom	30,892,000	1.67	0.42	515,896	417,151
Wanagon	24,500,000	na	2.68	na	2,111,050
Wanagon (skarn)	2,400,000	1.94	0.95	46,560	73,305
TOTAL	**3,030,741,000**			**36,549,144**	**108,666,437**

Values from Harrison (2000). na=grade not available, assumed to be negligible. Note that Kucing Liar constitutes the second largest concentration of copper and gold in the district. There are currently no other economically viable resources in Irian Jaya outside the Ertsberg Mining District. Regional exploration followed by intensive delineation activities conducted by PT Freeport Indonesia has identified 8Moz of gold in the Wabu deposit associated with the Wabu Pluton, 35km to the northwest of the Ertsberg mining district (Sunyoto, 2000) that is currently considered subeconomic.

1.1 Regional and local setting

1.1.1 Geology of New Guinea and the Southern Central Ranges

New Guinea lies immediately to the north of Australia and includes a number of distinct topographic and tectonic zones. The main island is defined by a prominent mountain belt which extends the length of the island and possesses a number of peaks with elevations over 4,000m. The island of New Britain lies east of the New Guinea mainland while the Melanesian Volcanic Arc lies outboard of New Britain and includes New Ireland, Buka-Bougainville and Solomon Islands, and broadly parallels the Papuan Fold Belt (Figure 1-4). Deep sea trenches lying to the south of New Britain and to the west of Bougainville reach depths >8,000m. A shallower trench, 3,000-4,000m deep lies outboard of the Melanesian Volcanic Arc.

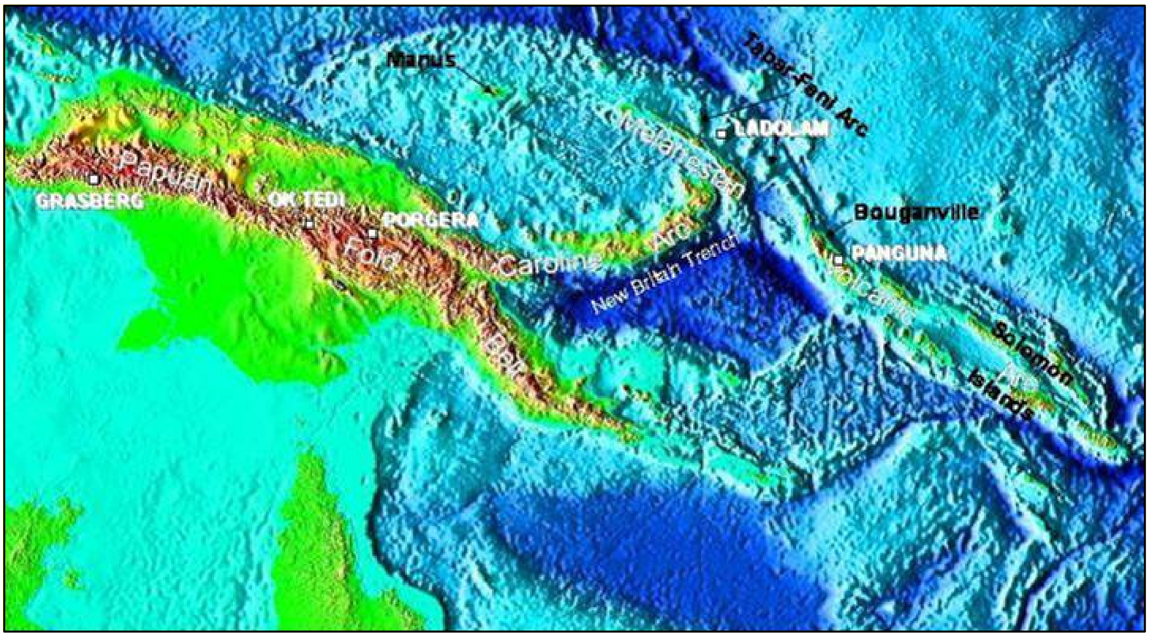

Figure 1-4 Physiography of Irian Jaya and Papua New Guinea

This digital elevation image shows New Guinea's extreme topography both above and below sea level. The Papuan Fold Belt is shown in orange and red colours of >1,000 and reaches >4000 in many locations, while the dark blue New Britain deep sea trench reaches depths of >8,000m. The locations of major porphyry-related deposits are indicated (image is a partial reproduction of picture acquired from website http://www.ngdc.noaa.gov/mgg/image/2minsurface/1350/00N135E.jpg, annotations added by author).

Tectonic evolution of New Guinea

The Papuan Fold Belt is the result of collision between the Australian continental plate and the Caroline and Pacific oceanic plates, which involved accretion of an island arc and ophiolite emplacement (Quarles van Ufford, 1996; Sapiie *et al.*, 1999; Warren, 2000; Hill *et al.*, 2002). The Jurassic age Irian Jaya ophiolite was emplaced along the northern margin of the Papuan Fold Belt (Figure 1-5). In Irian Jaya, the Derewo Metamorphic Belt separates accreted terranes from the sedimentary sequence of the Central Range. While the metamorphism of the Irian Ophiolite occurred during the Eocene (55-34Ma), metamorphism of the Derewo belt was initiated ~15Ma later in the late Oligocene (34-24Ma) to early Miocene (24-5Ma) (Weiland, 1999). Inclusion of metamorphic fragments in sediments of the Central Range indicates the Miocene development and denudation of a metamorphic fold belt (Weiland, 1999), which is indicated on Figure 1-5 by the development of a metamorphic core complex. South-directed subduction of the Caroline Plate ended in the Miocene (Solomon, 1990) and reversal to a north dipping subducting slab (Solomon Plate) beneath the easternmost remnants of the Caroline Island Arc (New Britain) occurred in the Pliocene (Figure 1-5). The Marumuni Arc developed in response to collision and accretion of the Caroline Island Arc along the northern margin of proto-New Guinea. The Pliocene magmatic arc on the New Guinea mainland developed in conjunction with the formation of the New Guinean Orogenic Belt (Papuan Fold Belt) (Figure 1-5). The current tectonic structure of the island changes in character and orientation from west to east. Irian Jaya is dominated by transcurrent faulting and stalled subduction, the middle part by transcurrent faults and slow convergence, and the eastern part by spreading ridges and active subduction (Figure 1-6a). Current tectonic activity is expressed by seismic activity and reveals a pattern of epicentres in which the deepest events are concentrated in belts that parallels plate contacts, particularly the New Britain subduction trenches, with decreasing depths westward. Only the shallowest earthquakes occur in Irian Jaya (Sapiie et al., 1999). Porphyritic intrusions have been emplaced along the axis of the Papuan Fold Belt (Figure 1-6b). Two temporally distinct igneous suites on the mainland were intruded during Miocene (20-7Ma) and Plio-Pleistocene (<7Ma) times into the evolving collision environment and form curvilinear arcs parallel to the elongation of the island and the tectonic plate boundaries (Figure 1-6b) (McDowell *et al.*, 1996). The older magmatic system is referred to as the Maramuni Arc while the younger is simply referred to as the Pliocene Arc. Both are areally restricted but more widespread in Papua New Guinea than in Irian Jaya (Figure 1-6b). Significant copper-gold mineralisation is restricted to the Pliocene Arc. Intrusions related to mineralisation in Papua New Guinea are both younger (e.g. Ok Tedi) and older (e.g. Porgera) than the age of intrusions in the Ertsberg Mining District (Figure 1-6b). Pliocene volcanoes are dotted about the mainland and adjacent island chains, including New Britain, Bougainville, and the Tabar-Feni chain outboard of New Ireland. On the mainland, volcanoes are noticeably clustered about the central Highlands as well as in lowland locations on the Papuan peninsula. Active vulcanism continues to the present data in the islands off eastern New Guinea as evidenced by the explosion and extensive ash deposition from volcanoes near Rabaul in 1996.

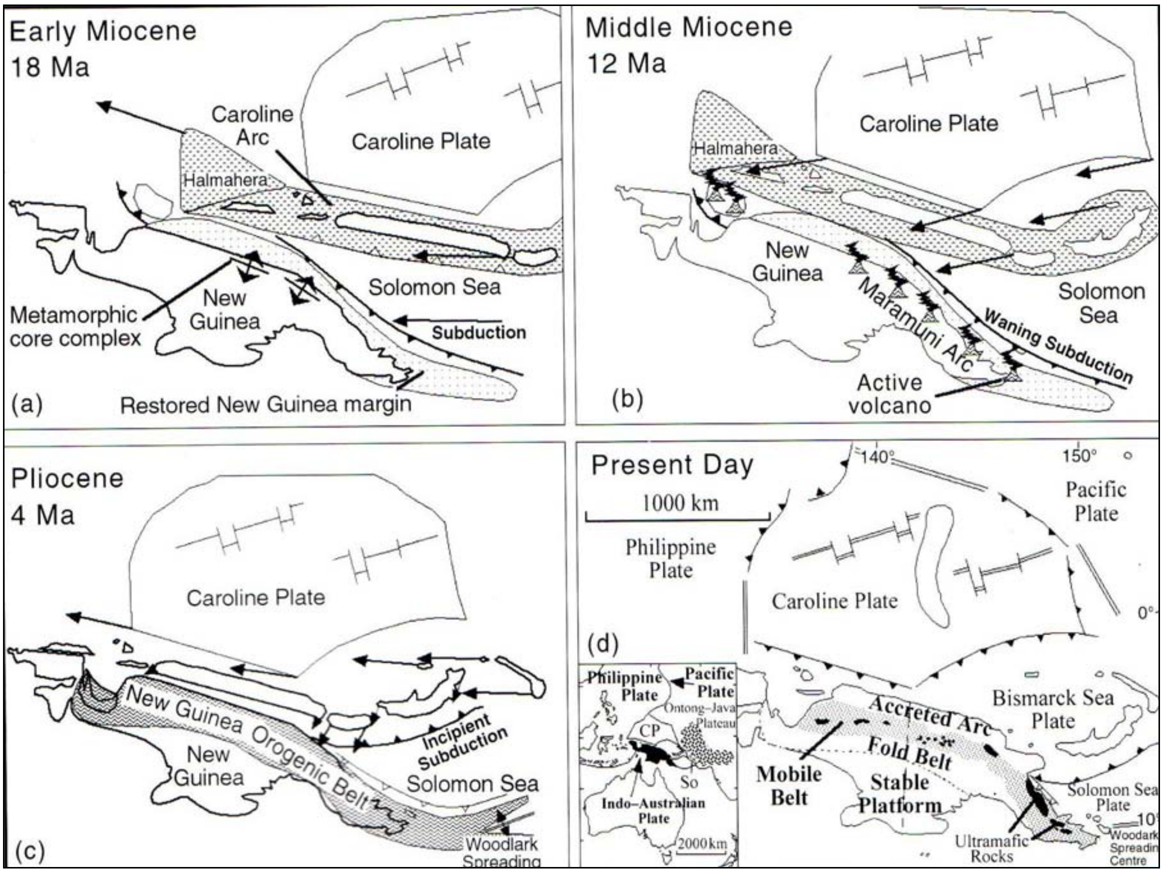

Figure 1-5 Palimspastic reconstruction of the evolution of New Guinea

A series of sketches illustrates the most significant events in the development of New Guinea and the age at which each event occurred. Reproduced from Figure 2 of Hill et al., (2002).

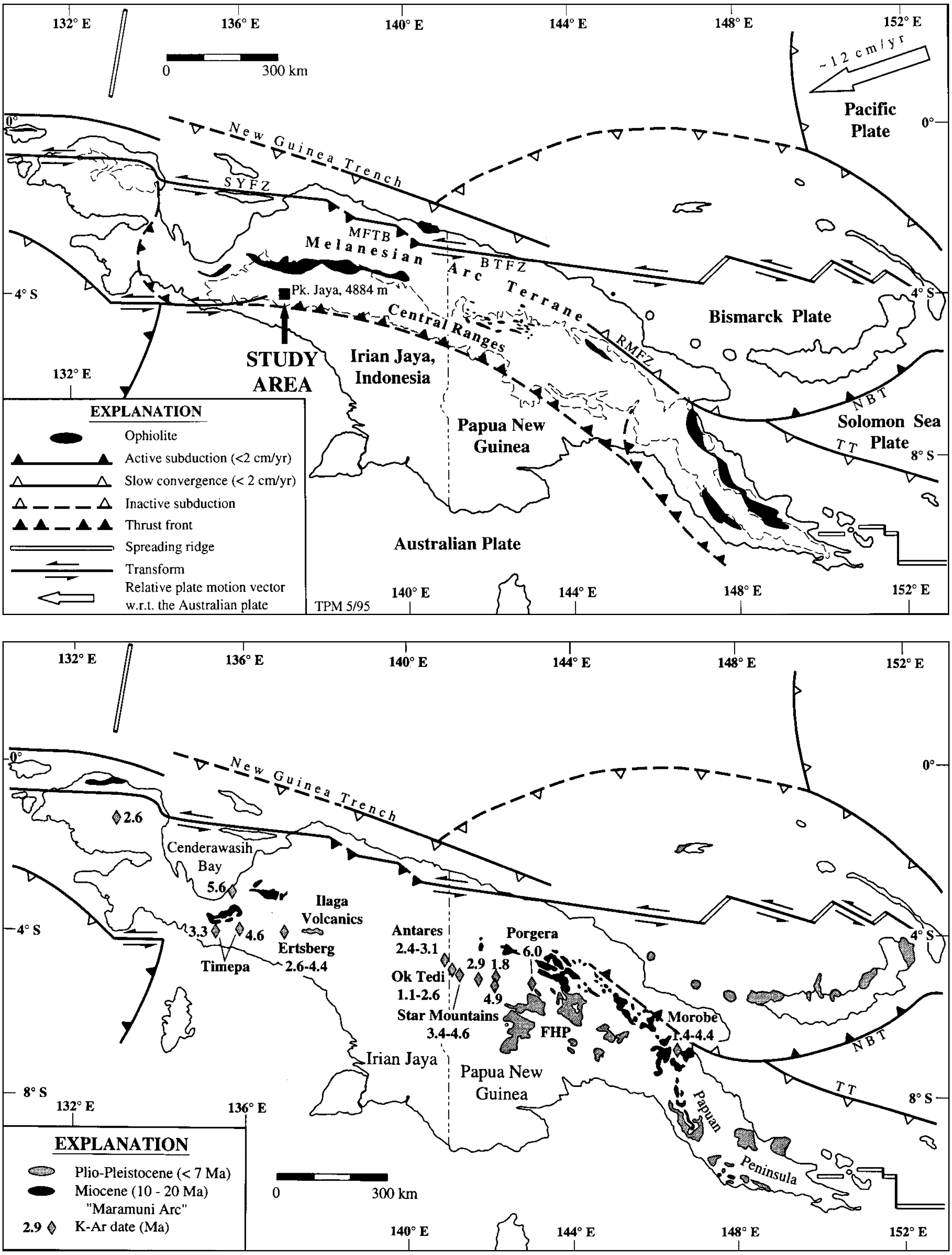

Figure 1-6 Tectonics and igneous intrusions of New Guinea (reproduced from McDowell *et al.*, 1996)

(a) Current convergence of the Pacific Plate is in west-southwest direction and subduction is restricted to eastern island arcs in the vicinity of New Britain and Bouganville. BTFZ = Bewani-Torricelli fault zone; MFTB = Mamberamo fold and thrust belt; NBT = New Britain trench; RMFZ = Ramu-Markham fault zone; SYFZ = Sorong-Yapen fault zone; TT = Trobriand Trough. (b) The Ertsberg mining district is indicated by the K-Ar age determination samples labelled "Ertsberg".

Stratigraphy and structure of the Southern Central Ranges

Collision tectonics in Irian Jaya have produced kilometre-scale folds and bedding-parallel sinistral strike-slip faults in the Ertsberg Mining District (Parris, 1994; Quarles van Ufford, 1996). In the vicinity of the Ertsberg Mining District, the sedimentary strata that comprise the mountain range are folded into a broad central syncline along the axis of the ranges. The stratigraphic sequence of the southern half of the Central Range now tilted and exposed along the road from Timika to Tembagapura (Pennington, 1995) reveals a sedimentary pile that was laid down discontinuously from Cambrian to Recent times (Figure 1-7). Thicknesses of stratigraphic units are consistent along strike (east-west) but vary across the axis (north-south) of the fold belt (Figure 1-7). Regionally, sedimentary strata are continuous along strike for hundreds of kilometres (Figure 1-8). The stratigraphic sequence here correlates with similar units in Papua New Guinea (Hill *et al.*, 2002). The strata in the Southern Ranges of Irian Jaya include thick sequences of mudstone, sandstone, limestone and dolostone ranging in age from Cambrian to Tertiary (Figure 1-7). Proterozoic pillow basalts at the base of the tectonic section are metamorphosed to lower greenschist facies and are strongly foliated in places. Mesozoic strata in the Ertsberg Mining District have equivalents in Papua New Guinea, but there are no Palaeozoic strata exposed in Papua New Guinea, where Mesozoic strata are underlain by granitoids and metamorphic rocks (Hill *et al.*, 2002).

In Irian Jaya, the mountain range associated with the Papuan Fold Belt is referred to as the Central Range, and the mountain-forming event is named the Central Range Orogeny (Quarles van Ufford, 1996). The Central Range fold and thrust belt is marked at its southern margin by a thrust fault named the Mapenduma Thrust and to the north by the Derewo Metamorphic Belt (Figure 1-8). The southern Central Ranges is an area of tilted and folded Australian continental margin sediments lying between two thrust faults which separate the Papuan Fold Belt from the Derewo Metamorphic Belt to the north and flat-lying margin sediments to the south. A sharp change in topography marks the location of the Mapenduma thrust. The Central Range between the Mapenduma Thrust and the Derewo Metamorphic Belt is dissected by oblique faults, which visibly offset stratigraphy with a left-lateral sense of displacement (Figure 1-8). These arc-oblique faults are traceable for long distances on the map and connect between the Derewo and Mapenduma Faults (Figure 1-8). They are accompanied by faults with much shorter lengths that are subperpendicular to the fold belt and have a left-lateral sense of displacement. A third set of faults strikes east-northeast but is not as well defined by stratigraphic offsets as the arc-oblique and arc-normal faults. The Ertsberg Mining District is associated with arc-oblique faults though less clearly associated with arc-normal faults (Figure 1-8). Igneous intrusions and volcanic fields are also related to east-northeast striking faults as demonstrated by the Ilaga Volcanic Field lying to the east of the Ertsberg Mining District (Figure 1-8). Mineralised intrusive bodies are also associated with thrust faults as demonstrated by the relationship of the Wabu Pluton with the Derewo Fault (Sunyoto, 2000), within the Derewo Fault (Figure 1-8).

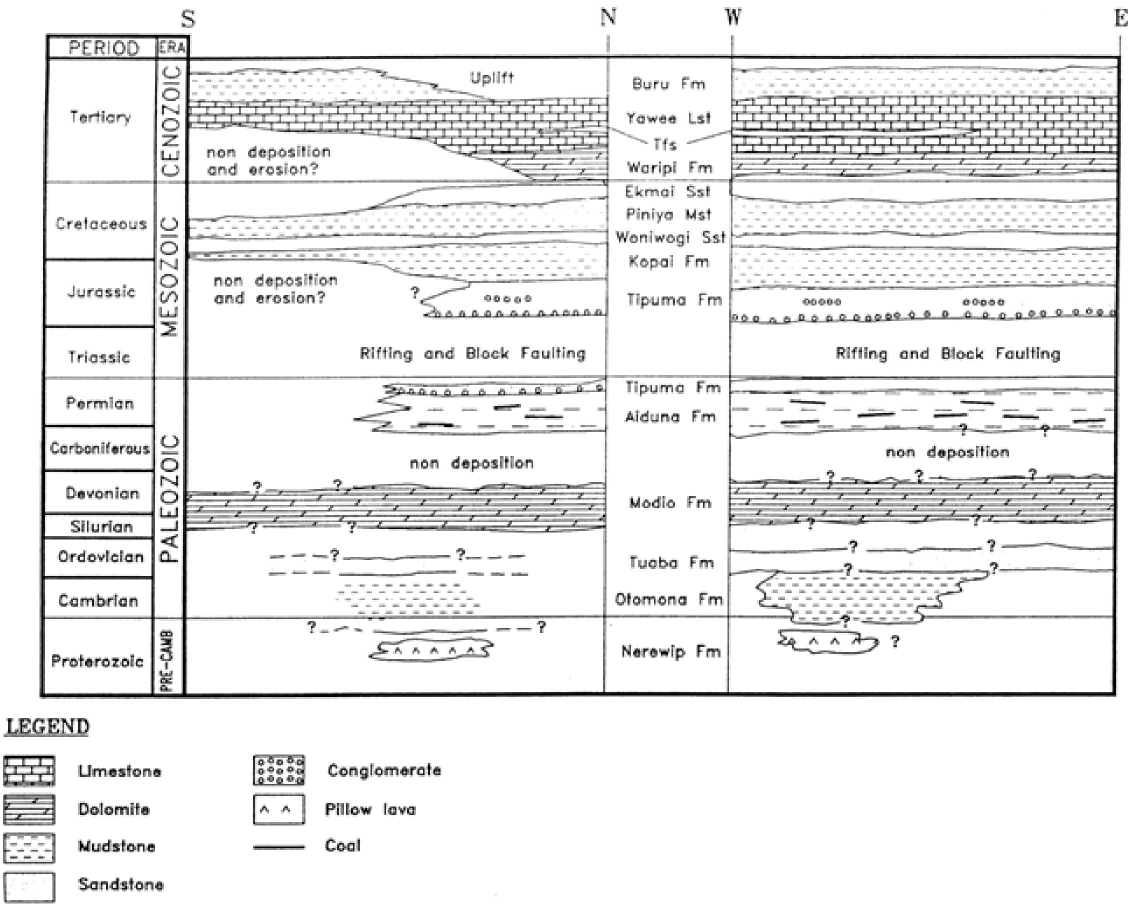

Figure 1-7 Sedimentary record of the Timika-Tembagapura region (reproduced from Parris, 1994a).

The section indicates lateral continuity from east to west along the continental margin but variable thicknesses from north to south, perpendicular to the margin.

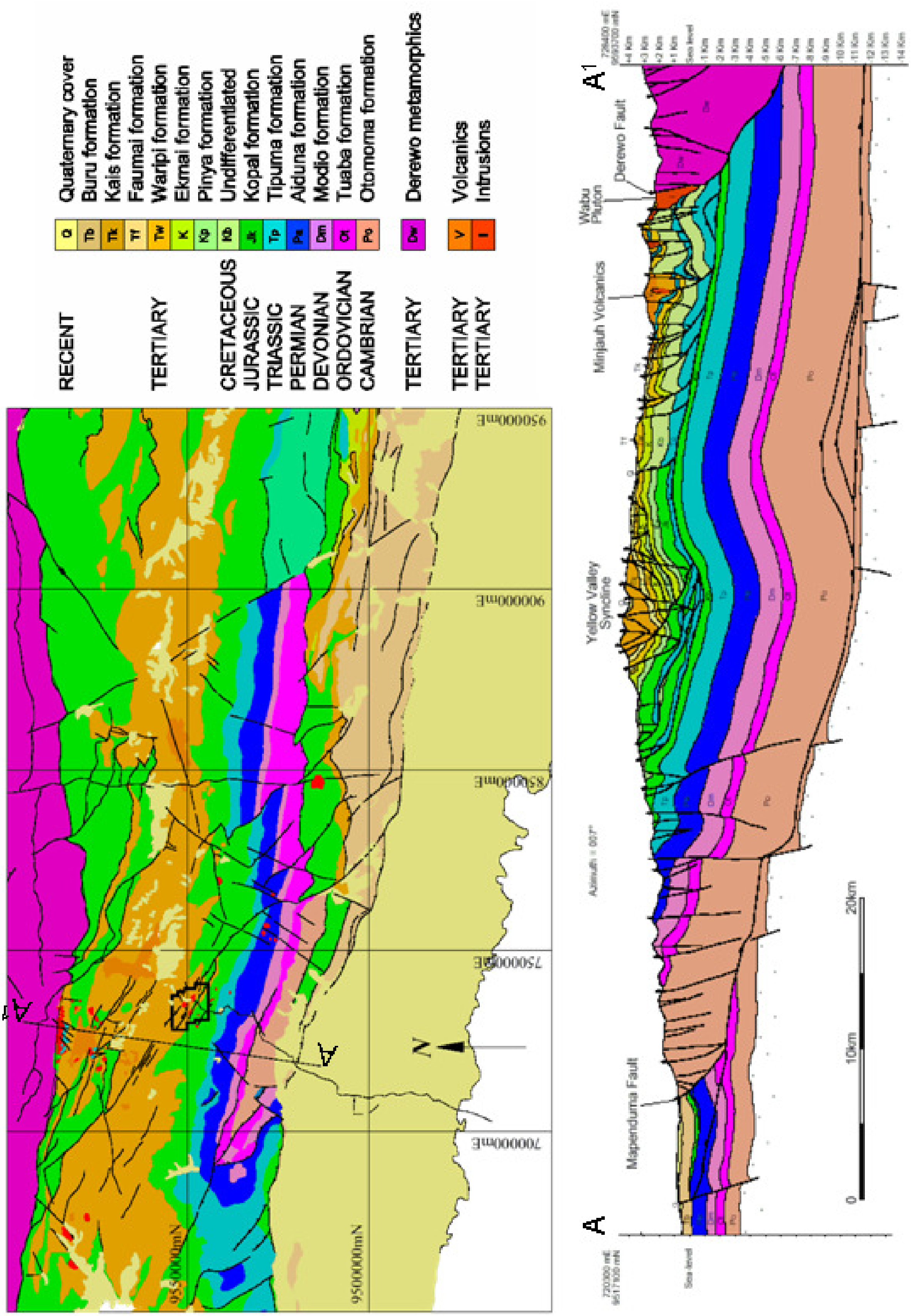

Figure 1-8 Geology of southern flanks of the Central Range

Black box = CoW A (Contract of Work, block A). Map modified from Parris (1994b).

1.1.2 Geology of the Ertsberg Mining District

The geology of the Ertsberg Mining District has become well understood due to local, district and regional research programs on tectonostratigraphy (Quarles van Ufford, 1996; Weiland, 1996), structural controls (Sapiie, 2001), intrusive bodies (McMahon, 1996), and individual deposits (Macdonald and Arnold, 1994; Mertig et al., 1998; Meinert et al., 1998; Widodo *et al.*, 1998; Pollard and Taylor, 2002; Prendergast, 2004). Units in the mine district have experienced ~5km of uplift associated with 100km-scale-shortening manifest in large-amplitude folds and high angle reverse faults (Quarles van Ufford, 1996). The district includes the axial zone and southern limb of the regional-scale Yellow Valley Syncline (YVS) that is cross cut by arc-parallel, -oblique and -normal faults. The Yellow Valley Syncline trends parallel to the Central Range and plunges shallowly northwest (Figure 1-9). The northern and southern limbs have been disrupted by steeply dipping bedding parallel faults that have displaced the core of the syncline upwards relative to the limbs.

Tectonostratigraphic data for Irian Jaya (Quarles van Ufford, 1996; Sapiie *et al.*, 1999) record a history of folding and reverse faulting from 12-4Ma followed by left lateral fault movement between 4-2Ma. Symmetric and asymmetric repetition of stratigraphic marker horizons such as the Sirga sandstone and the Tk2 layer within the Kais Limestone (Figure 1-9) indicate that both folding and thrusting has occurred. Major thrust displacement is apparent along the Wanagon Fault. In addition to thrust faulting, left lateral movement is documented for the large faults in the Ertsberg Mining District that trend subparallel to stratigraphy (Sapiie, 2000; Sapiie and Cloos, 2004). These strike-slip faults (Wanagon, Idenberg Nos 1 & 2, Ertsberg Nos 1, 2 & 3) have reported displacements of 1,500m (Figure 1-9). Other faults are visible and strike northeast to east-northeast. This set of faults has smaller apparent left-lateral displacements and includes the New Zealand Pass Fault and the Grasberg Fault, which intersects the Yellow Valley Syncline in the vicinity of the Grasberg Igneous Complex (Figure 1-9).

Igneous units in the Ertsberg Mining District have been intruded as columnar and elongate bodies into the axis and limbs of the Yellow Valley Syncline in the form of the Grasberg Igneous Complex and the Ertsberg Intrusive Suite (previously described as undifferentiated Ertsberg porphyry). The Grasberg, Kay and Lembah Tembaga intrusive complexes have near circular outcrop pattern (though the latter occurs beneath Lake Wanagon), while the Ertsberg and Wanagon intrusions are elongate parallel to the main strike (see Figure 1-9). The Grasberg Igneous Complex (GIC) occupies the axis of the Yellow Valley Syncline where it is intersected by the high angle Grasberg Fault. The Ertsberg Intrusion is controlled by the Ertsberg No1, No2 & No3 faults to the east and the Idenberg No1 & No2 faults to the west (Figure 1-9). Similarly, the Wanagon Sill appears to be related to the position of the Wanagon Fault. The Kali dykes are the youngest intrusive phases and appear to have intruded into the centre of the Grasberg Igneous Complex parallel to the axis of the Yellow Valley Syncline. These intrusions were emplaced at ≤2km, and sourced from depleted mantle with small contributions from an ancient, enriched mantle reservoir (McMahon, 1994b; Housh and McMahon, 2000). They are divided into a high-K group (latites, trachydacites and trachytes) and a low-K group (medium to high-K andesite and dacite); the high-K group includes the Grasberg Igneous Complex and Ertsberg Intrusive Suite (McMahon, 1994a; McMahon, 1994b).

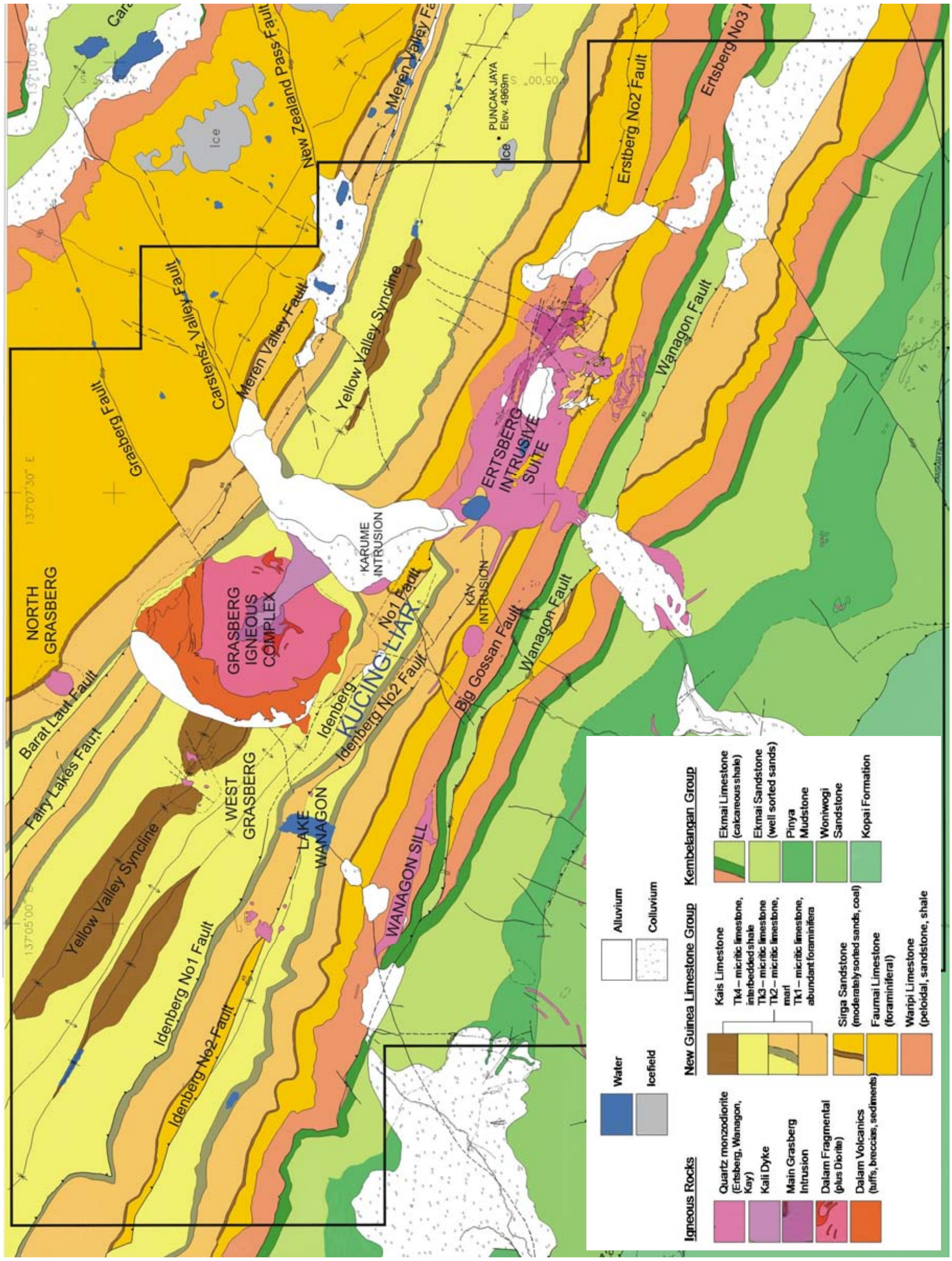

Figure 1-9 Geological map of the Ertsberg Mining District (supplied by PT Freeport Indonesia)

Cretaceous units are shown in green colours and Tertiary units in brown; intrusions are red to pink coloured. Kucing Liar is adjacent to the Grasberg Igneous Complex, and along strike from the Ertsberg Intrusive Suite to the east and the Lembah Tembaga (beneath Lake Wanagon) porphyry intrusion to the west.

1.2 ACCESS AND METHODS

1.2.1 Physiography of the mining district

Kucing Liar is situated within the Erstberg Mining Distict near the watershed of the Central Ranges of West Papua. The Ertsberg Mining District was originally centred on the Ertsberg deposit, and occupies roughly 100km^2 of the deeply incised south flank of the Central Ranges of Irian Jaya. The mine site lies at, and above the vegetation line. Ice accumulations fringe mountain peaks just 5km from the mine site, that in the past were true glaciers flowing directly past the present mine site, just 4°S of the equator (Quarles van Ufford and Sedgwick, 1998). The district boundary, originally square, was altered to exclude icefields which are now part of the adjacent Lorentz nature reserve, which covers a large area from the middle of the Central Range to the low-lying areas adjacent to the ocean. Topography in the mine district is severe (Plate 1-1) with elevation ranging from 2,000m to 4,880m. The northern boundary of the district is in the highest elevations of the Central Ranges mountain belt which reaches its maximum of ~4,884m at the nearby peak of Puncak Jaya. Mining in the district was originally concentrated on the Ertsberg deposit before moving to the Ertsberg East Skarn System (EESS), which continues to supplement the current primary mining activity at Grasberg. Both Ertsberg and Grasberg are open pit mines while the EESS is mined via large-scale underground block caving methods. Grasberg mineralisation is centred on the Grasberg Igneous Complex while four deposits are situated at the periphery of the Ertsberg Intrusion hosted by sedimentary rocks, namely the Ertsberg, Ertsberg East, Dom and Big Gossan skarn systems.

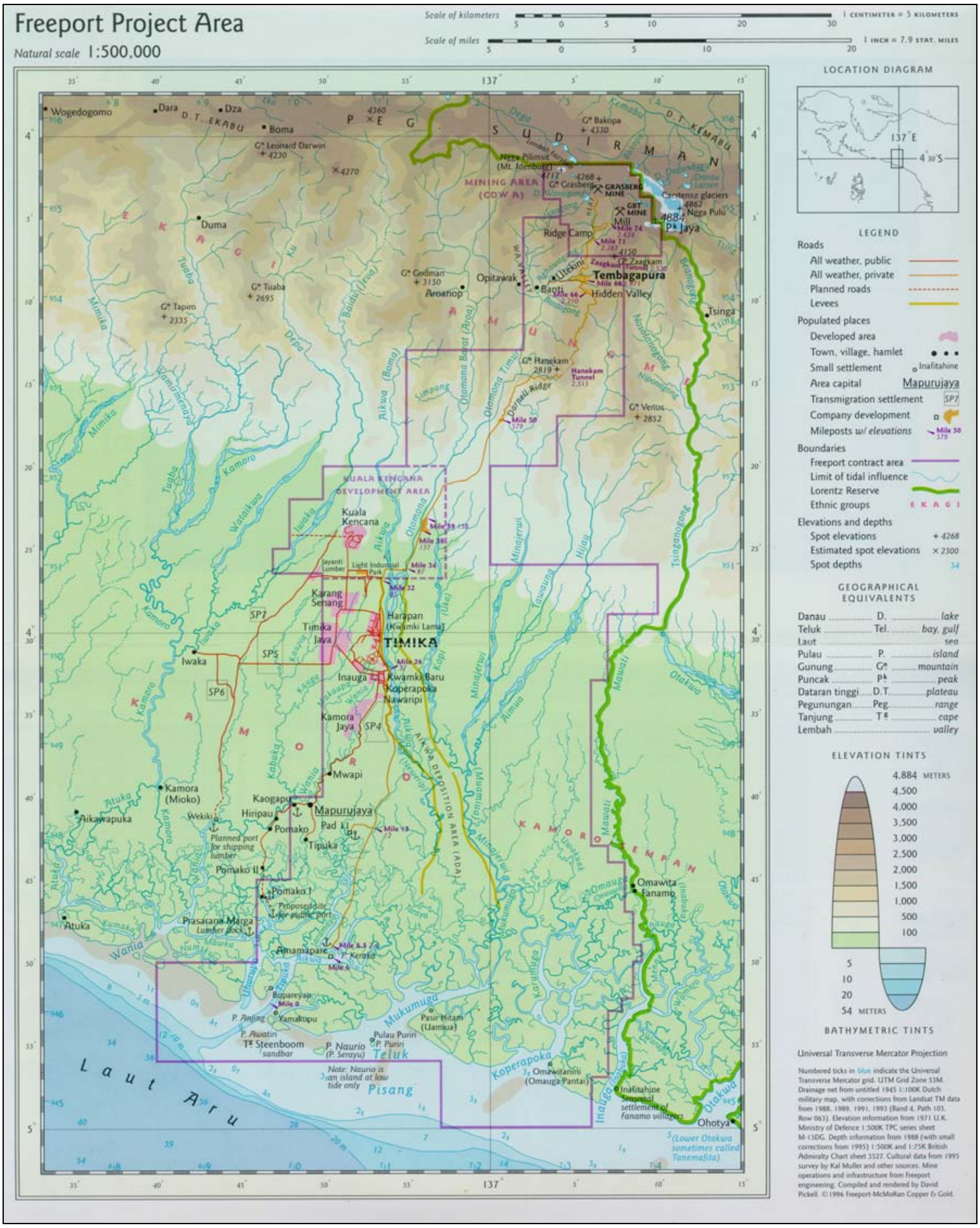

Figure 1-10 Physiography of the Southern Ranges and Ertsberg Mining District

A plan of the regional geography and operational infrastructure of the Ertsberg mining district. A road constructed by Freeport connects the port of Amamapare, the airport town at Timika, the mine town of Tembagapura and the mill site over a distance of 124km, reaching an elevation of 2,800m. Ice fields, formerly glaciers are visible at upper right of the figure coloured white and blue. There are mile distances and spot elevations in metres included along the road connecting the port to the mine site. Reproduced from Mealey (1996).

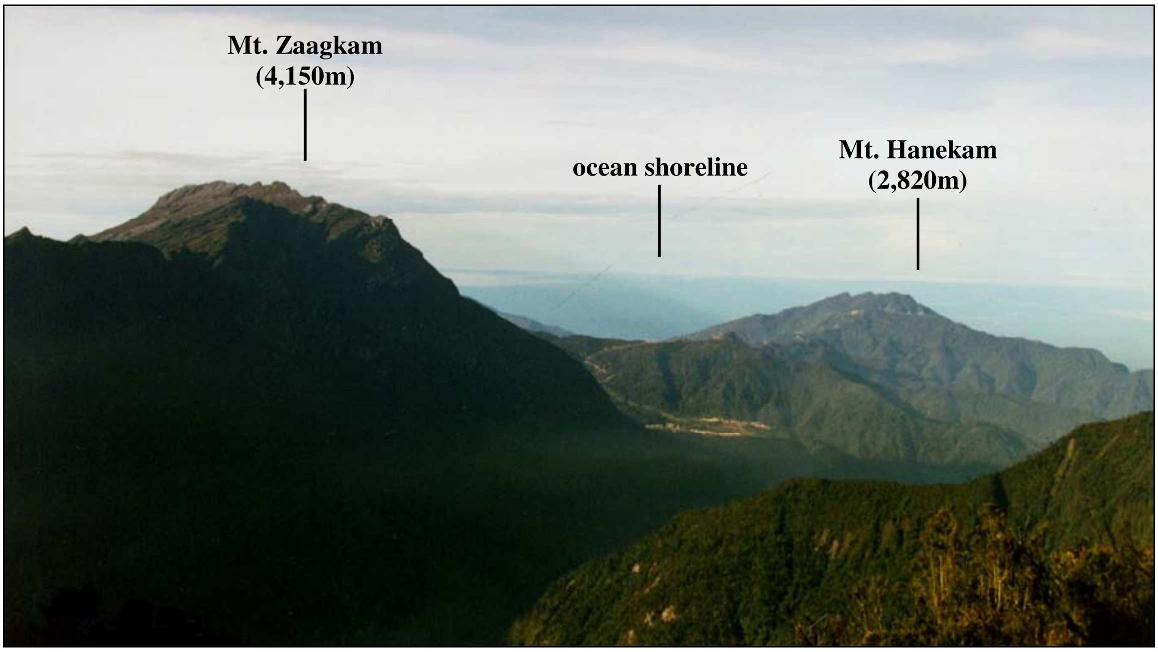

Plate 1-1 Relief of the Ertsberg Mining District and access routes

(a) View looking south from the Ertsberg Mining District between the 4,150m Mt Zaagkam and the 2,820m Mt Hanekam. The collection of buildings visible at lower centre is Hidden Valley, perched at the top of the steep-sided valley where Tembagapura is located. The access road connecting Timika, Tembagapura and the mill site is visible tracking along ridge tops between Mt Zaagkam and Mt Hannekam. (b) A view looking east toward Puncak Jaya, the highest mountain in Southeast Asia. The Grasberg open pit mine operations are to the left of view. The Heavy Equipment Access Trail (HEAT), which provides access to the mine, is visible in foreground. The Kucing Liar deposit occurs at depth below the north-south trending ridge in the middle of picture, with the Big Gossan skarn deposit located further to the south (right). Power pylons are perched on smaller ridges in the foreground of this ridge.

1.2.2 Sources of data

A detailed history of exploration and mining in the Ertsberg Mining District, including initial exploration for Kucing Liar is included in the book *Grasberg* (Mealey, 1996). Kucing Liar, meaning “wild cat” in the Indonesian language, was actively explored for in favourable sedimentary units adjacent to the Grasberg Igneous Complex following discovery of mineralised country rock fragments at the margin of the Grasberg Igneous Complex in 1992 and high-grade intersections during deep exploration in 1994 (Macdonald, *pers. comm.*). The Grasberg Igneous Complex is a wineglass shaped body composed of multiple igneous bodies in its stem and of heavily fragmented zones overlain by layered pyroclastic rocks in the flared upper zone. A tunnel driven at 3000mRL into the Grasberg Igneous Complex from the mill to control water influx into the Grasberg open pit intersected significant mineralisation associated with a fault and was given the name Amole, meaning, “welcome” in the local Amungme language. A second level driven northwest subparallel to the dominant strike of stratigraphy provided a platform for delineation of this zone by diamond drilling (Figure 1-11). Drill stations spaced evenly along strike confirmed that the Amole mineralised zone was contiguous with Kucing Liar (“wild cat”) intersections some 800m further west on the access trail to Grasberg. Excavations spaced at 50m intervals along this drive were completed for drilling stations, of which 16 were originally completed spaced 100m apart covering 1,500 metres of regional stratigraphic strike (Figure 1-12). Later infill drilling was conducted in the centre of deposit to confirm continuity of the resource at a distance of 50m, the core from these holes have been inspected but not included in the dataset for the current research project. Drilling was conducted in radial patterns on azimuths of 39 or 219° (Figure 1-12), perpendicular to the regional strike (Figure 1-13). Collar positions and downhole survey orientations for all drilling are recorded in Appendix 1.

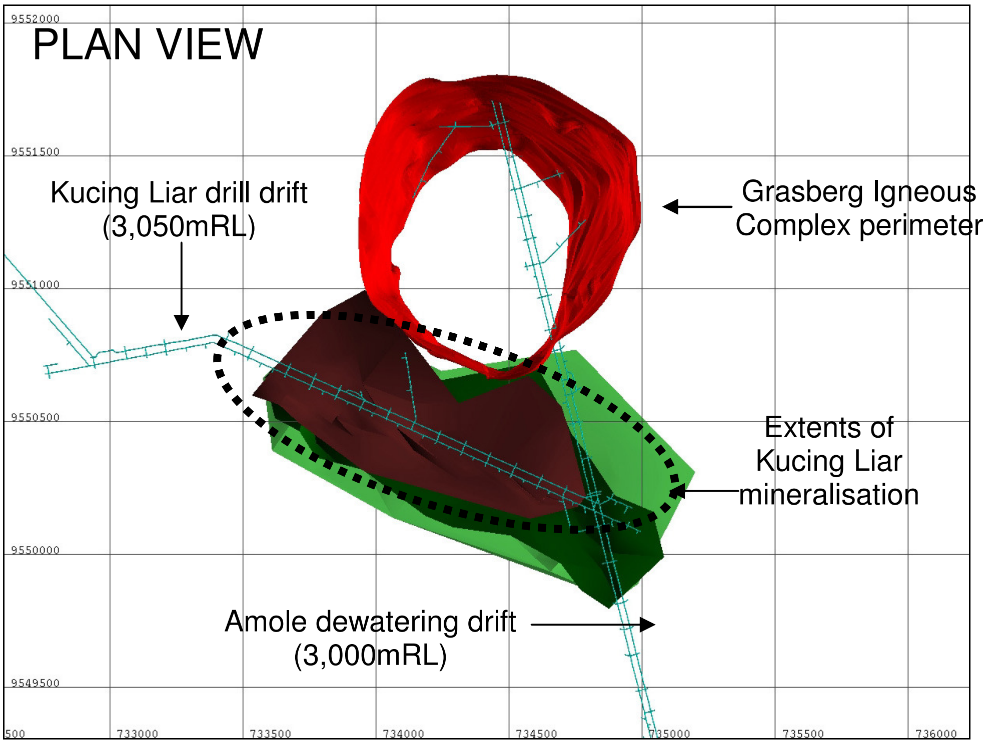

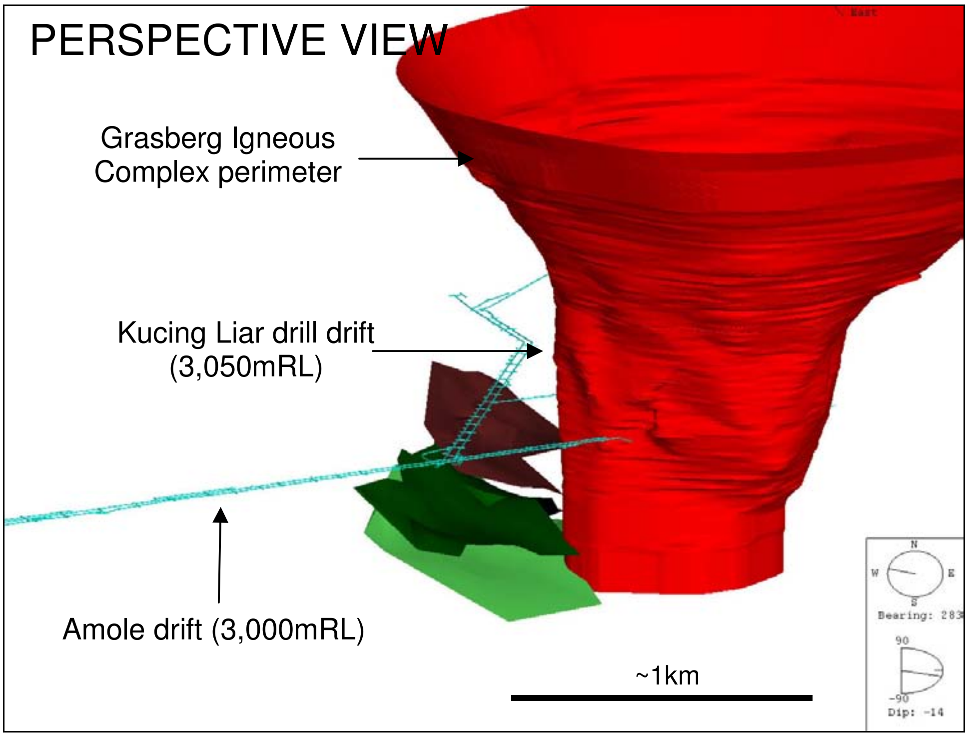

Figure 1-11 Position of Kucing Liar mineralisation relative to Grasberg Igenous Complex

Plan and perspective views illustrate the location of Kucing Liar with reference to Grasberg as well as dewatering and delineation tunnels. The outer perimeter of the Grasberg Igneous Complex (supplied by Peter Manning of PT Freeport Indonesia) is coloured red while the Kucing Liar mineralised zone is represented by three surfaces representing major internal stratigraphic contacts that are coloured brown, dark green and light green. Underground access levels are shown in light blue. The perspective view has no vertical exaggeration.

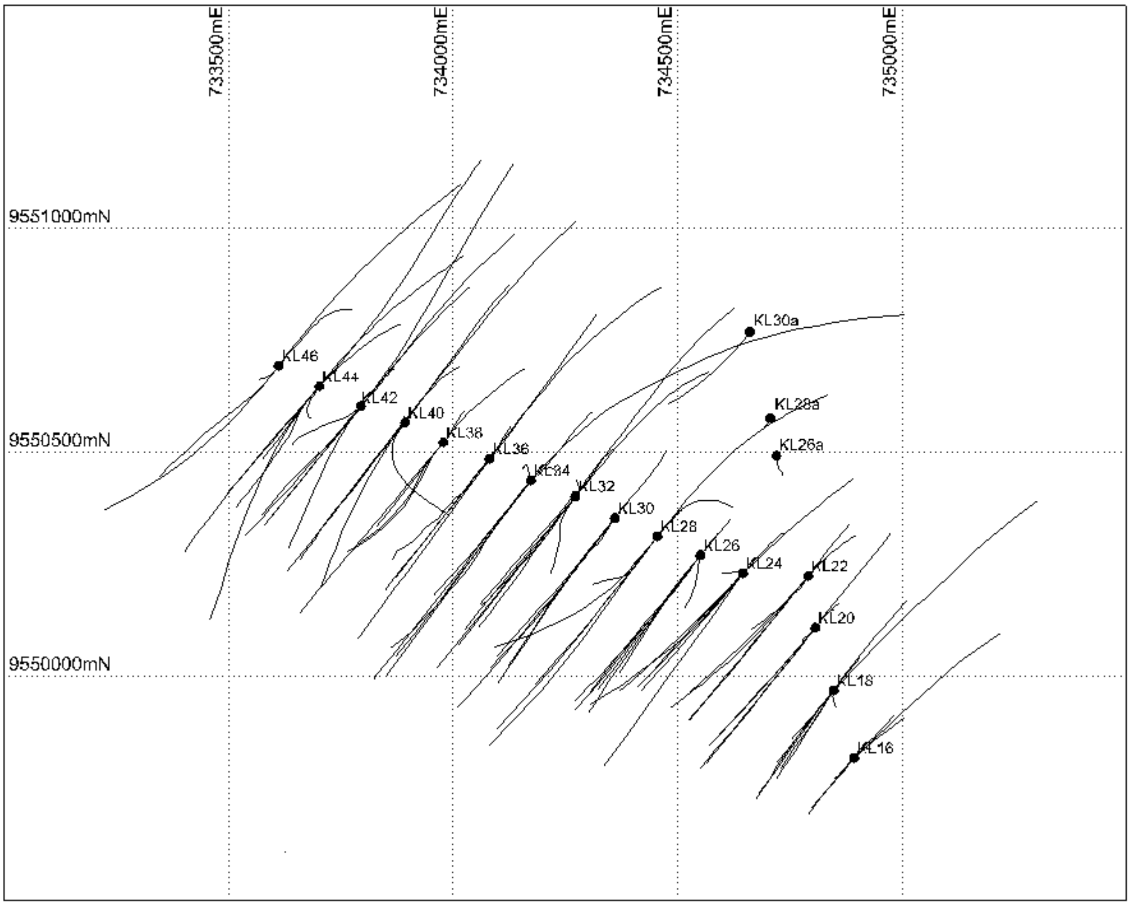

Figure 1-12 Plan view of all Kucing Liar drill traces logged for this research program

Plan view of drilling including all holes sampled and measured for this research program. The traces of drilling are projected in plan view and many overlie each other. The filled circles represent the location of the collars and the drill station position. Compare with Figure 1-11. The drill stations are labelled with the prefix KL, followed by the station number and a number exclusive to each hole (eg. KL16-03, KL32-04). KL26-11, KL28-9 and KL30-9 were collared from the Amole dewatering drift. The dip and azimuth of each drill hole have been surveyed every 3m on average and this data has been used to position each interval.

Holes were nominally divided into 3m lengths by PT Freeport Indonesia geologists for assaying but shortened if a change in geology was identified. A short length of drill core (10-20cm) was removed from each assayed interval and retained, producing an archive of "skeleton" core. All of the drill holes in Figure 1-12 and Figure 1-13 were logged using these samples on two separate occasions from Sept.-Nov. 1997 and June-Sept. 1999. The second period of logging revisited many of the drill holes logged on the first occasion. Due to the location and the extreme elevation (Plate 1-1), no field mapping was conducted for this research project, though one visit was made to a baseline stratigraphic section that was considered equivalent to the Kucing Liar host rocks.

Figure 1-13 Layout of all holes in each drill station logged for this research program

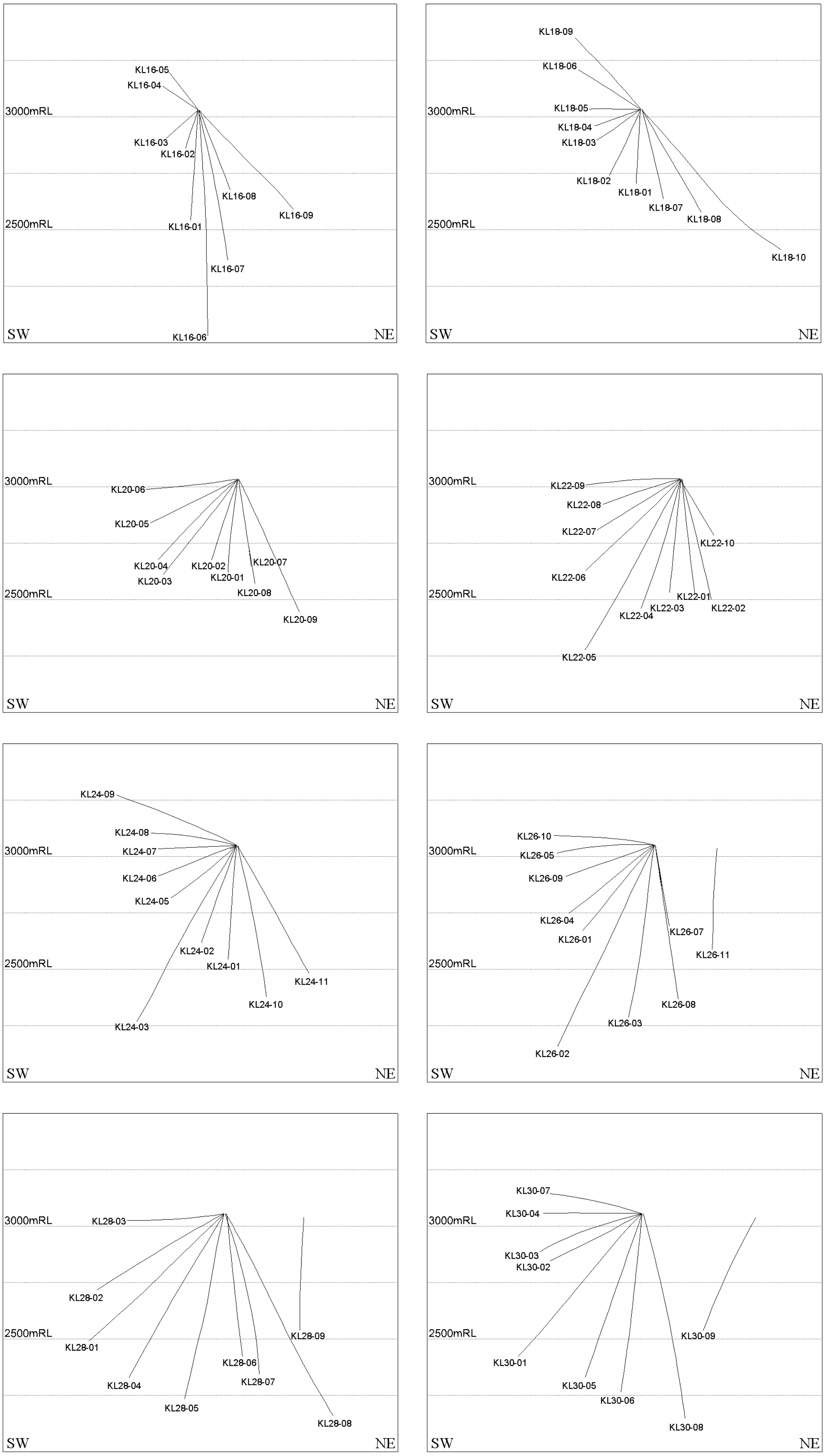

Figure 1-13 Layout of all holes in each drill station logged for this research program (cont.)

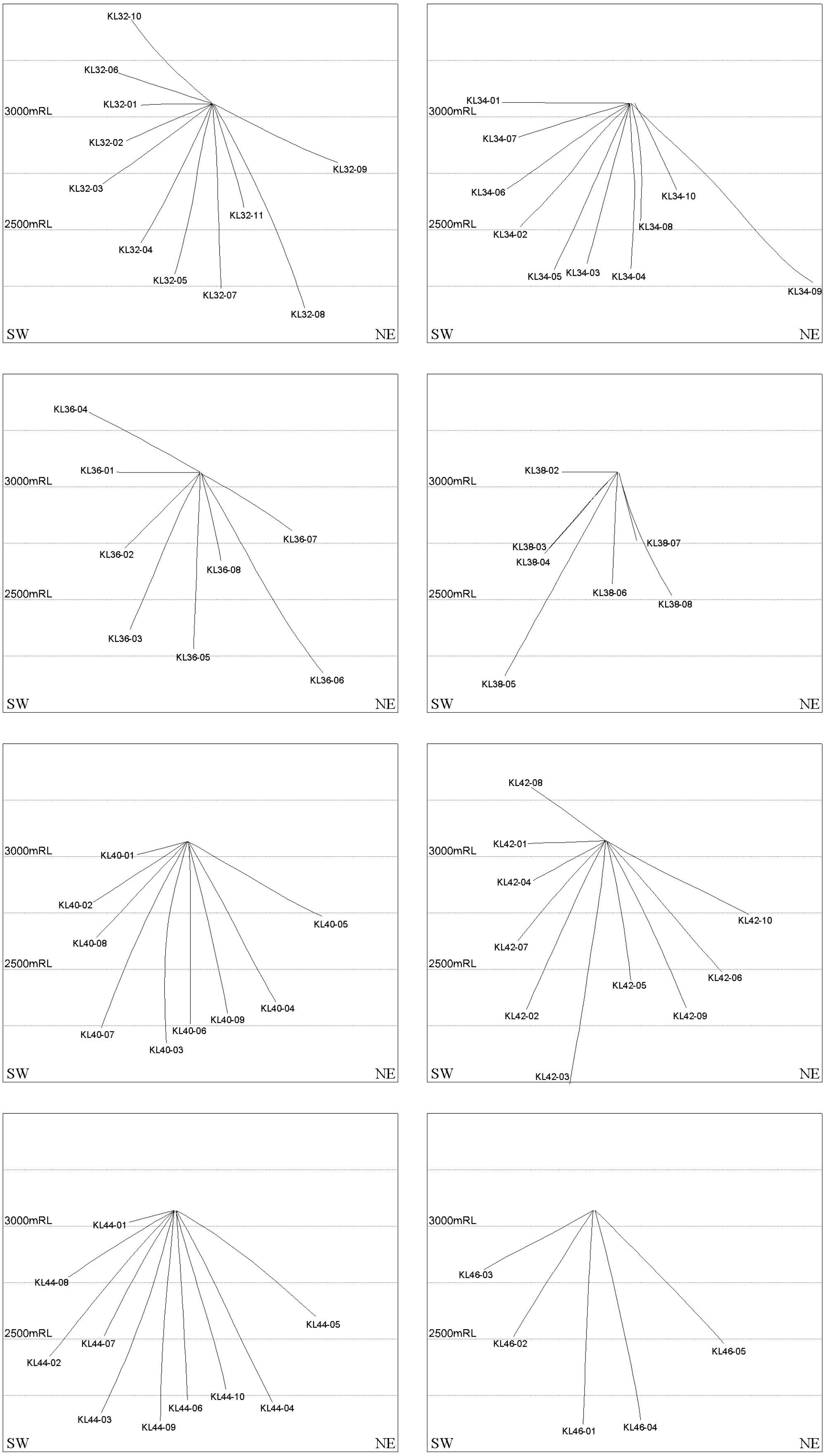

2 Host rocks

This section documents the wall rocks hosting Kucing Liar in terms of their composition and stratigraphical sequence. Each unit of the stratigraphic sequence is described in terms of lithology and internal sequence. The division of stratigraphy followed here is in line with that currently used within the mine environment by PT Freeport Indonesia. The rocks found in relatively unaltered sequences were compared to distinctive samples from the main mineralised zone in order to determine the reliability of textures observed in mineralised specimens for interpreting the stratigraphic position of individual samples (Chapter 4).

2.1 Previous work and sources of data

2.1.1 Regional stratigraphic sequence

The stratigraphic sequence in the Ertsberg Mining District represents a continental margin including tidal, inner and outer shelf, plus deep marine sediments (Table 2-1). The Kembelangan Group is the lowermost stratigraphic package and comprises thick monotonous accumulations of shale and sandstone deposited in dominantly marine conditions from middle Jurassic to late Cretaceous times (Pennington, 1995; Quarles van Ufford, 1996). Contacts with both the underlying terrestrial to shallow marine Tipuma Formation and the overlying marine New Guinea Limestone Group are described as conformable (Pennington, 1995; Quarles van Ufford, 1996). The overall thickness of the Kembelangan Group is cited as 4,600m ± 1000 (Quarles van Ufford, 1996), while Pennington (1995) indicates that although the exposed thickness along the road exceeds 3,400m, the actual thickness is only 1,900m. The discrepancy is thought to be the result of tectonic thickening. The Kembelangan Group is subdivided into four formations, namely, the Kopai Formation, Woniwogi Sandstone, Pinya Mudstone and Ekmai Sandstone. Internal contacts have been described as conformable to disconformable by Quarles van Ufford (1996) but as conformable by Pennington (1995). In this study only the uppermost unit of this group, the Ekmai Sandstone, is significant. It is ~600m thick and is constrained by fossil evidence to a middle-upper Cretaceous age though it may possibly extend into the Palaeocene (Pennington, 1995; Quarles van Ufford, 1996). The upper Ekmai Sandstone is a 120m thick carbonaceous limestone referred to by mine geologists as the Ekmai Limestone, which includes an uppermost layer referred to as the Ekmai shale. Neither of these units was differentiated by Pennington (1995) or Quarles van Ufford (1996) but they are included on local geological maps (Parris, 1994).

The New Guinea Limestone Group conformably overlies the Kembelangan Group, is unconformably overlain by Quaternary glacial sediments and is documented as being 1,600-1,800m thick (Pennington, 1995: Quarles van Ufford, 1996). The sequence defines a regressive-transgressive-regressive sequence indicated by lower and upper platform carbonates separated by fluvial and tidal facies sediments. The New Guinea Limestone group is subdivided into the Waripi Limestone, Faumai Limestone, Sirga Sandstone and Kais Limestone which were deposited on a stable carbonate platform marine over a ~50Ma period from latest Cretaceous to middle Miocene times (Quarles van Ufford, 1996). The Waripi Limestone is described as being 250-300m thick and is assigned a Palaeocene to early Eocene age (Pennington, 1995). The presence of anhydrite nodules within this unit indicates emergent conditions and supratidal environments. The upper contact with the overlying Faumai Limestone is described as conformable and gradational while the lower contact with the Ekmai Limestone may be disconformable (Pennington, 1995). The Faumai Limestone is distinguished from the Waripi Limestone by the presence of foraminifera and by the lack of sandstone (Table 2-1). The lower contact is conformable with the Waripi Limestone while the upper contact with the Sirga Sandstone is unconformable (Pennington, 1995), though evidence of prolonged exposure of the unit was not found (Quarles van Ufford, 1996). The Sirga Sandstone is a transgressive sequence of fluvial or near-shore sandstones including some organic-rich beds. The uppermost Kais Limestone is further subdivided into separate members, referred to by mine geologists as Tk1, Tk2, Tk3 and Tk4 (Parris, 1994). Although the top of the Kais Limestone is not exposed, the unit is at least 1,100m thick (Quarles van Ufford, 1996). It is distinct in the district as having a unique texture derived from tightly packed, large and elongate foraminifera. The lower contact with the Sirga Sandstone is conformable, while the upper contact is an erosional unconformity.

Table 2-1 Descriptions of stratigraphy in the Ertsberg Mining District

Formation	Lithology	Depositional environment
Kais Limestone (Tngk) 1,100 – 1,300m	Red algal, benthic foraminiferal limestone to packstone at the base, well developed bedding but internally massive. Massive, fossiliferous marls layers in lower sections.	Restricted shallow-marine carbonate platform sheltered from open marine currents
Sirga Sandstone (Tngs) 40m	Fining-upwards trough and tabular cross stratified quartz arenite, reworked foraminifera, coal and plant-rich seams.	Transgressive from terrestrial to shallow-marine and subaerial exposure, fluvial or nearshore unidirectional depositional current
Faumai Limestone (Tngf) 200 – 300m	Benthic foraminiferal limestone and packstone, 10m thick sandstone in lower and middle sections, occasional dolomite.	Shallow marine carbonate platform, restricted medium-energy
Waripi Limestone (Tngw) 250 – 400m	Sucrosic dolostone, quartz arenite sandstone and 2m thick nodular anhydrite-bearing beds.	Transitional from siliciclastic to carbonate, high energy shallow-marine shelf
Ekmai Sandstone (Kkes) 650m / 600m	Variably grain-sized quartz arenite with trough and tabular cross-bedding, upper 90m is mudstone and limestone.	Shallow shelf, nearshore to possible beach facies, the upper limestone is outer-shelf to slope
Pinya Mudstone (Kp) 1550m / 600m	Laminated massive mud and siltstone interbedded with 20cm thick well-sorted and fine-grained sandstone.	Shelf margin and slope during transgression, storm generated sands and fair weather mud.
Woniwogi Sandstone (Kw) 1000m / ~300m	Poorly-sorted coarse-gained to granule sandstone overlain by well-sorted fine to medium-grained sandstone, sporadic cross-bedding but generally massive; belemnites.	Shallow marine and slope from sand-rich shelf, basal section is either beach or debris flows
Kopai Formation (Kkp) 1400m / 300m	sandstone, siltstone/mudstone and subordinate limestone; crinoids, echinoderm and ammonite.	Transitional fluvial to nearshore marine, shallow shelf, distal shelf or slope. Lower sections are transgressive, upper sections are regressive

Source: Pennington (1995) and Quarles van Ufford (1996). The numbers below the unit names refer to their thicknesses. There is a consistent discrepancy between local and district studies where larger values are reported from regional studies.

2.1.2 District outcrop and deep drilling

There are numerous spectacular large-scale exposures of the Kucing Liar host stratigraphy in the district (e.g. Plate 2-1). The most visible differences in the stratigraphic units are the relative thicknesses of beds and the effects of erosion (Plate 2-1). The Ekmai Sandstone situated at the base of the mineralised sequence is very thickly bedded at a scale of tens of metres. By contrast, the overlying Waripi and Faumai Limestone units are very thinly bedded. A major topographic break occurs at the upper contact of the Ekmai Sandstone, which is suspected to be due to mechanical contrasts between the thick sandstone and thinner limestone, possibly exacerbated by the presence of the carbonaceous Ekmai Limestone. The contact of this unit with the underlying sandstone is very deeply eroded relative to overlying and underlying units in the walls of the Aghawagon Valley (Plate 2-1). Topographic breaks in the stratigraphic pile are consistent across the district and are situated at changes from sandstone to limestone or shale (Plate 2-1). These breaks have been used as marker horizons during district-scale geological mapping in defining the position of stratigraphic contacts (P. Manning, *pers comm.*). The extremely rugged nature of outcrop in the Ertsberg Mining District makes it logistically difficult to investigate. Consequently, analysis of strata intersected by exploration drilling at the margins of the Grasberg Igneous Complex (Figure 2-1) has provided details of the composition, texture and sequence of the Kucing Liar host sequence.

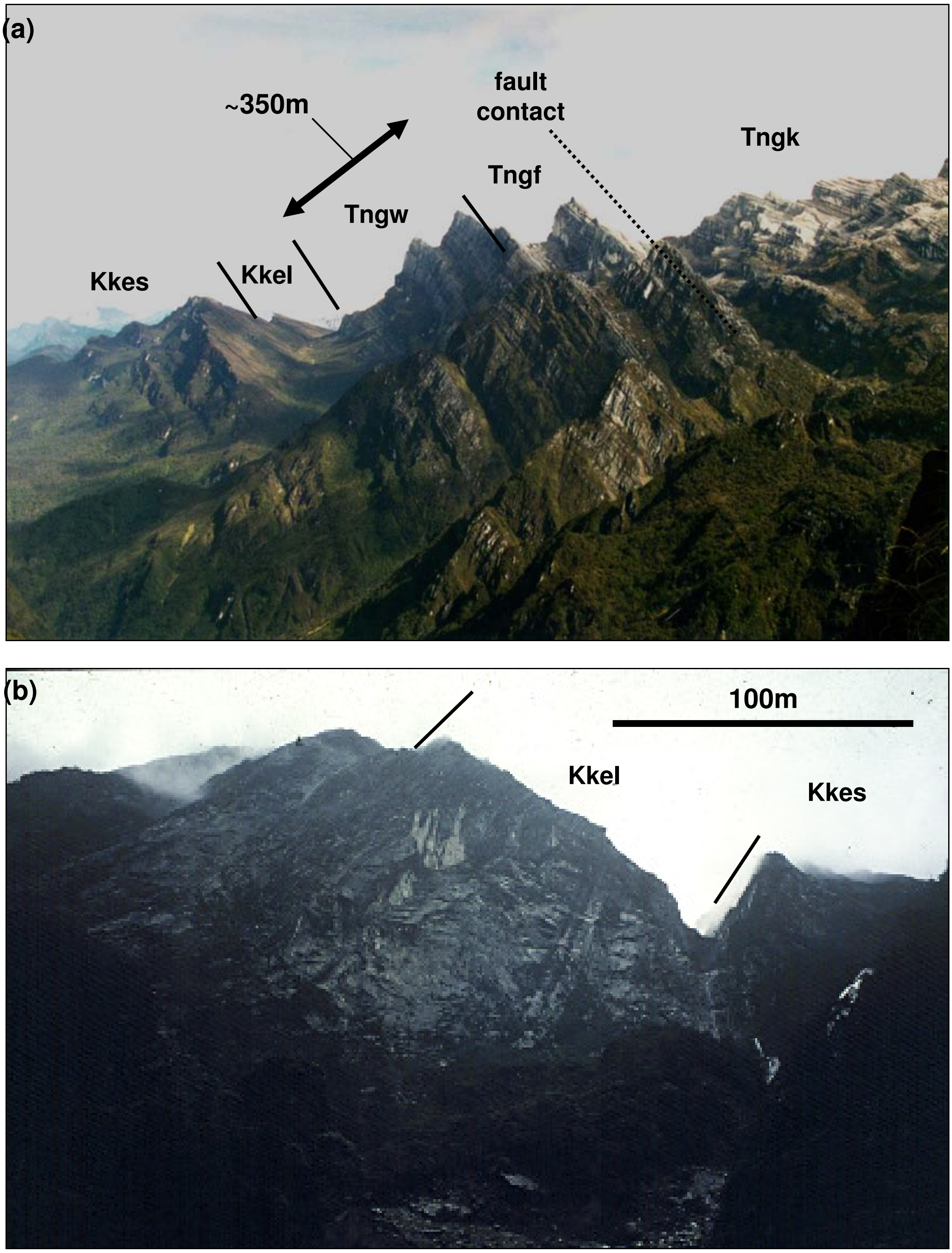

Plate 2-1 Large-scale exposure of host stratigraphy

(a) View west from north of Wanagon along strike showing a continuous section of stratigraphy. Breaks in topography are related to lithology, the most prominent occurring at the transition from Ekmai Sandstone (Kkes) to Ekmai Limestone (Kkel). Topographic breaks reflect visible changes in the bedding scale, which is small for the Waripi (Tngw), Faumai (Tngf) and Kais (Tngk) limestone units and much larger for the Ekmai Sandstone. The different dip of Kais Limestone to the right is probably due to faulting. (b) A view of the east wall in a valley where the mill is situated illustrates deep weathering of the Ekmai Limestone and a close up view of the thinly bedded Waripi Limestone.

Drilling conducted on the north and northwest margins of the Grasberg Igneous Complex intersected reasonably coherent stratigraphy equivalent to the host rocks at Kucing Liar. Mine staff identified the major stratigraphic packages and the contact characteristics prior to this study. Two drill holes, KLS1-1 (total depth 2199m) and KLS3-1 (total depth 2235m) completed in the course of district exploration intersected less altered equivalents of the Kucing Liar sequence, respectively northeast (northern limb of Yellow Valley Syncline) and northwest (axis of Yellow Valley Syncline) of the Grasberg Intrusive Complex (Figure 2-1). Drill hole KLS3-1 is near vertical and is expected to record true thicknesses of stratigraphic units as the stratigraphic layering should be near horizontal in the axis of the syncline. These two drill holes intersect the least altered host rocks available but nevertheless contain locally significant alteration. Although KLS3-1 was collared in the Grasberg Igneous Complex it intersected sedimentary units at 200m depth due to the flaring outwards of the igneous-sediment contact. No igneous bodies were intersected at depth in either of these drill holes. Drill hole KLS1-1 ended some 200m into the Ekmai Sandstone, while KLS3-1 intersected only the top 75m of the unit. KLS1-1 and KLS3-1 were both sampled for this study from the base of the Kais Limestone to the top of the Ekmai Sandstone at roughly 10m intervals, or less where significant changes in lithology were observed. Samples were collected from these two drill holes for petrographic examination and characterisation. Stained thin sections were produced to determine carbonate compositions of each sample. Details of the procedure are recorded in Appendix II. Carbonate composition is revealed in the colour imposed on the grains and matrix by staining. Dolomite is colourless to blue, while calcite is pink to purple. In each case, the darker colours are due to the presence of iron. Discrimination of calcite, dolomite, ferroan dolomite and ferroan calcite is possible from this technique. Thin sections were used to collect information specifically relating to:

- grain composition , size and abundance,
- matrix composition, grainsize and abundance, and
- carbonate composition.

Identification of foraminifera for the of the Faumai, Sirga and Kais units was facilitated by a report completed by the Palaeontology and Stratigraphy Division of the Geological Research and Development Centre, Directorate General of Geology and Mineral Resources, Department of Mines and Energy in Bandung, West Java (GRDC, 1999). Stratigraphic columns for each of the drill holes were created from the data recorded in thin section descriptions, allowing correlation of the major stratigraphic features (Figure 2-2).

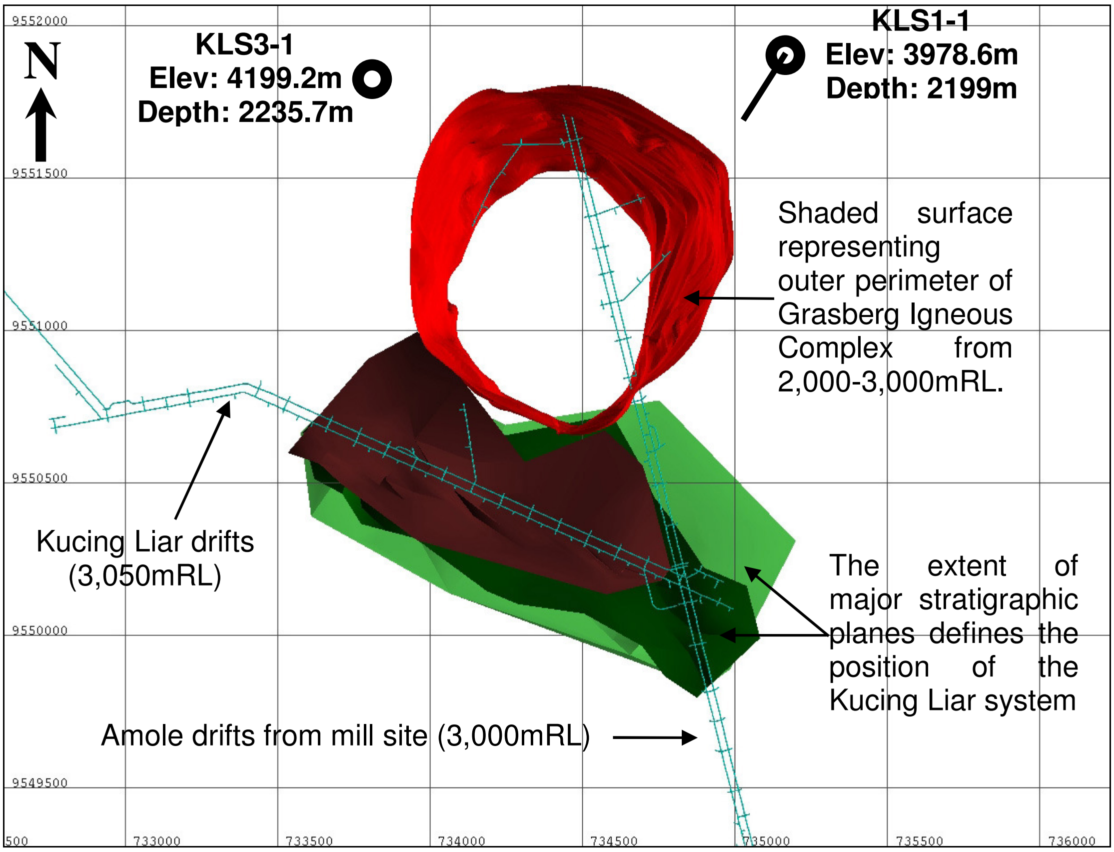

Figure 2-1 Plan projection showing collar locations for stratigraphical drillholes

Positions of KLS1-1 and KLS3-1 with reference to the location of Grasberg and Kucing Liar. KLS3-1 is vertical to the end of hole; KLS1-1 is vertical to 600m, then dips -60° toward southwest then is near vertical again from 900m. The section of KLS1-1 sampled for this study (870-2,200m) is oriented at -60° toward 213°. Grid spacing is 500m.

2.2 Results

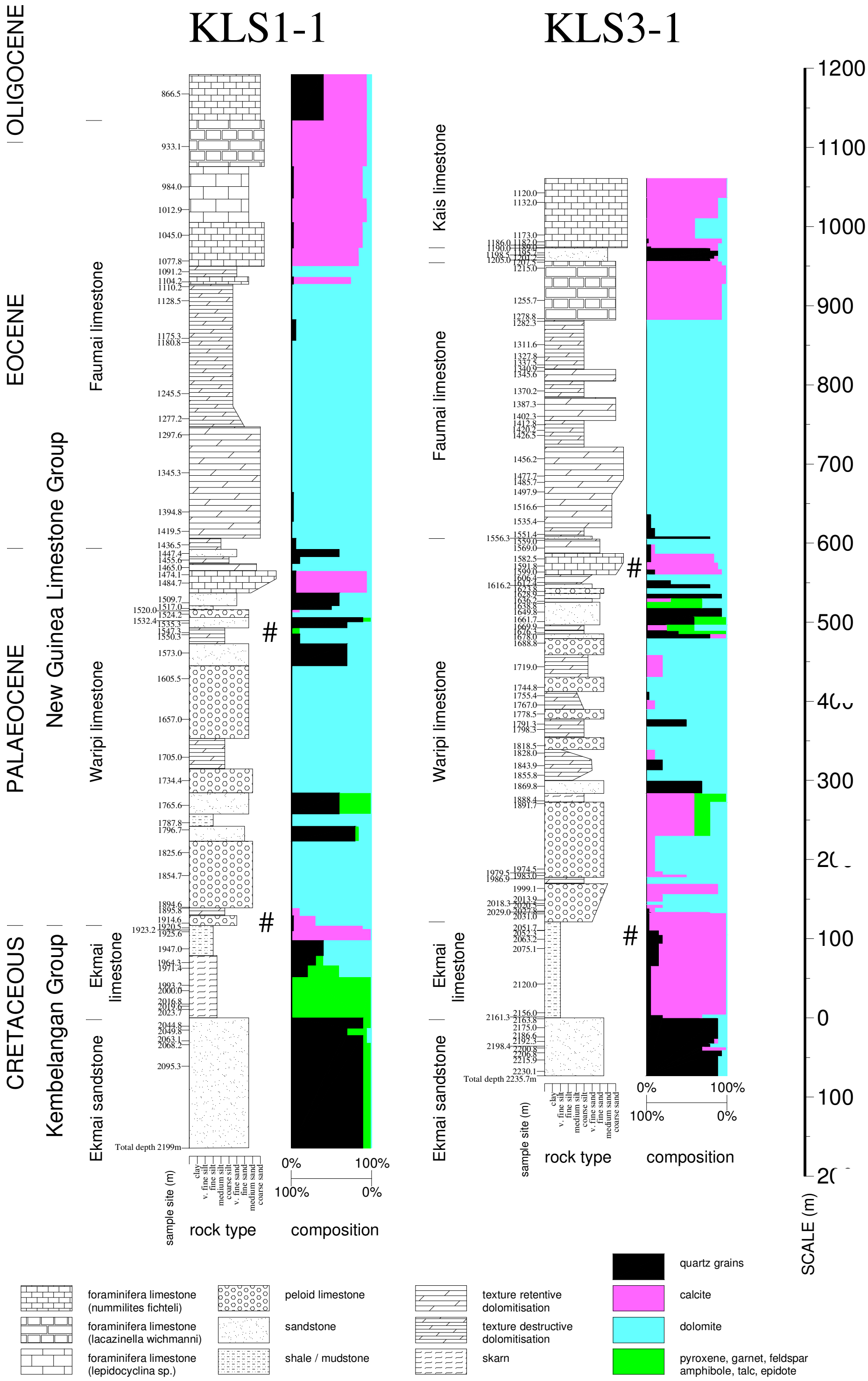

Figure 2-2 Lithology and composition of unmineralised stratigraphy

Sample locations from KLS1-1 and KLS3-1 for lithology descriptions are shown on the left of each column and marked by a tick and the depth. Different apparent thickness of the Faumai Limestone is due to variable intersection angles. Ages from Pennington (1995) and Quarles van Ufford (1996). Hatch symbols indicate presence of anhydrite nodules.

2.2.1 Descriptions of local unaltered lithological sequences

Kembelangan Group – Ekmai Sandstone (Kkes)

The Ekmai Sandstone is the lowermost unit intersected in Kucing Liar drilling. Its base was not intersected in either drill hole KLS1-1, which penetrated 170m, or in KLS3-1, which penetrated only 75m (Figure 2-2). The unit is largely homogeneous and consists of 80-90% very well sorted, angular to subangular quartz grains of 0.3mm grainsize and rare complete foraminifer (Plate 2-2a). However, there are also minor layers of red sandstone and coarse-grained bioclast-bearing sandstone (Plate 2-2b). The Ekmai Sandstone is thickly bedded (~50-100m) and bedding planes that are visible in large-scale exposures (Plate 2-1) are not recognisable in drill core. The overlying contact with the Ekmai Limestone is defined by disappearance of quartz grains (Figure 2-2).

Kembelangan Group – Ekmai Limestone (Kkel)

The Ekmai Limestone is 120m thick in KLS3-1 where it is almost pristine, while the intersection in KLS1-1 is altered to pyroxene-feldspar-garnet-epidote. The predominant lithology is very fine-grained black micritic limestone with a significant shale component containing up to 20% quartz and bioclasts. The base of the unit contains apparent bioturbation textures (Plate 2-2c). The limestone changes from massive and shaly in the lower sections, to fissile in the middle (Plate 2-2d), and bioclastic near the top (Plate 2-2e). A distinct layer (~5m) of black shale at the top of the Ekmai Limestone is locally referred to as the Ekmai shale.

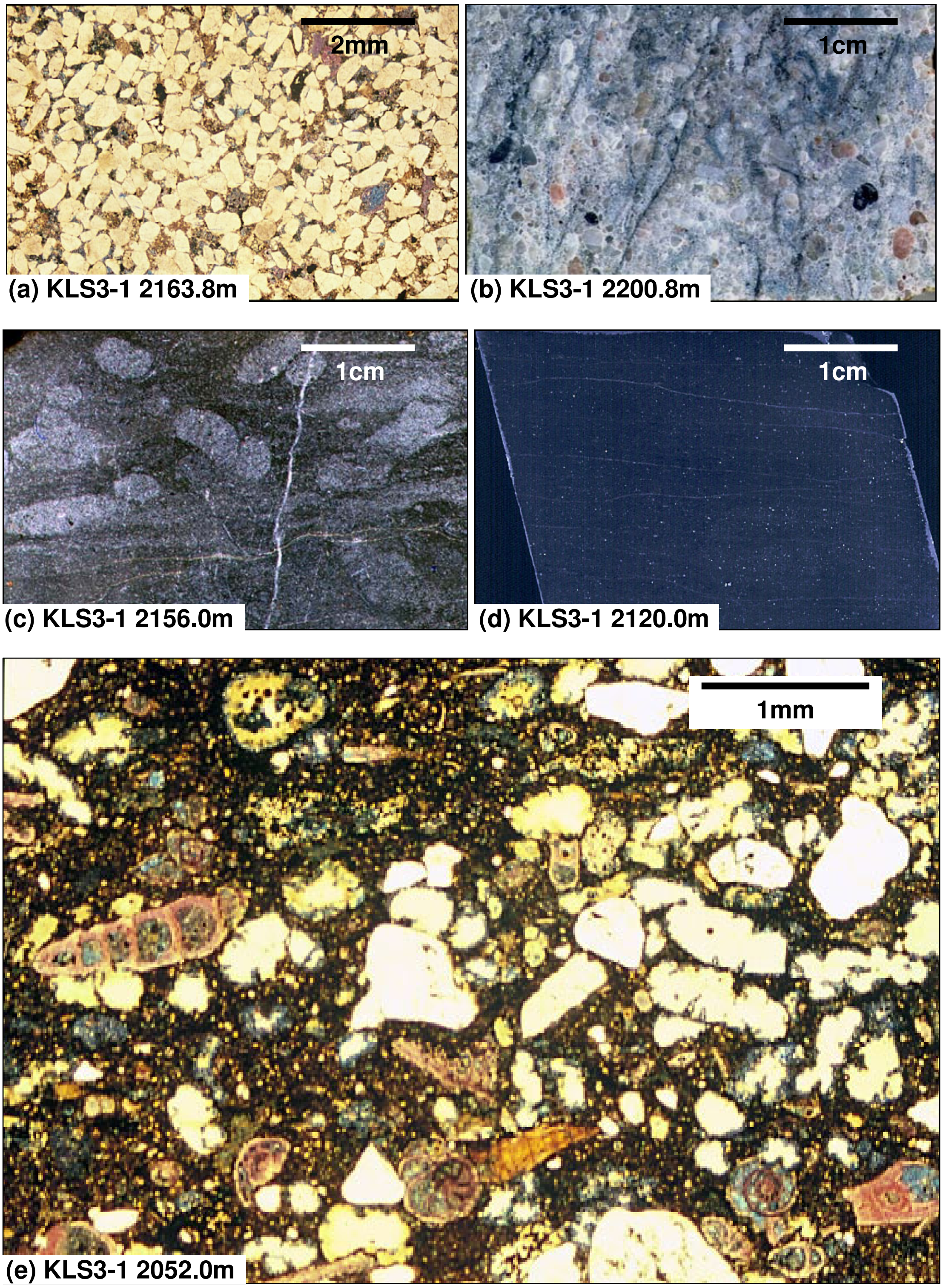

Plate 2-2 Examples of Ekmai Sandstone and limestone

(a) Photomicrograph of typical Ekmai Sandstone at the top of the unit, stained for carbonate composition. A grain (right) stained blue (ferroan dolomite) and pink (calcite) is a foraminifer. Plane light (b) Coarse-grained sand and carbonate layer (<5m) near top of Ekmai Sandstone. (c) Pale grey patches of sand grains in shale/limestone from the lower Ekmai Limestone that may be burrows. (d) Fissile shale from the middle of the Ekmai Limestone. (e) Coarse-grained texture of sand and bioclasts in a shale matrix of the upper Ekmai Limestone. Plane light image of a stained section.

New Guinea Limestone Group – Waripi Limestone (Tngw)

The Waripi Limestone is approximately 430m thick in KLS3-1, which is significantly more than the ~250m indicated by district studies (Pennington, 1995; Quarles van Ufford, 1996). It is dominated by peloid limestone but contains significant layers of sandstone, plus subordinate foraminiferal limestone and shale. The unit has been extensively dolomitised in both KLS1-1 and KLS3-1, although some samples containing primary calcite were collected. Exposed sections of the Waripi Limestone have very well defined sub-metre scale bedding structures (Plate 2-3).

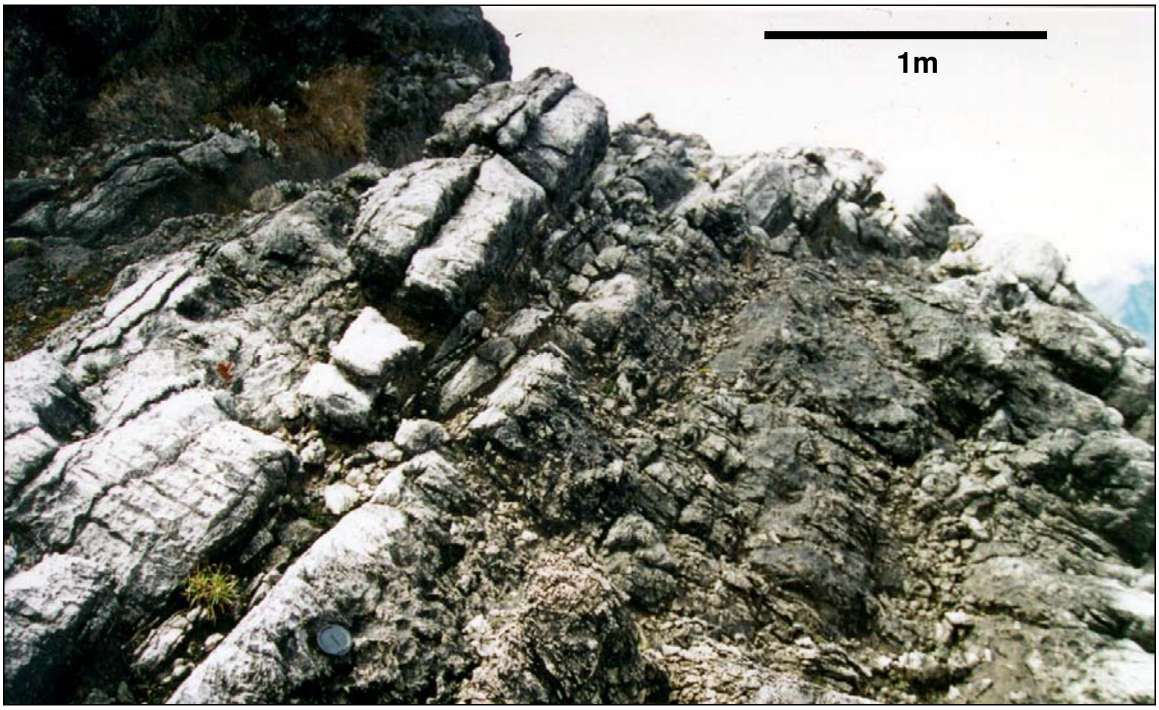

Plate 2-3 Outcrop of the Waripi Limestone

Layers of dolomite in outcrop of the section measured by mine staff near the Waripi Limestone-Faumai Limestone contact to the north of the Wanagon sill outcrop.

Grey peloid limestone/dolostone (Plate 2-4a) forms sections up to 180 thick in the Waripi Limestone (Figure 2-2). Peloid grains are spherical, micritic, possess no internal structure and constitute 60-80% of the rock. Peloid grainsize varies from 0.1 to 0.6mm but averages 0.3mm. Where peloid limestone is not dolomitised, the grains and matrix are composed of micritic calcite.

There are three sandstone members within the Waripi Limestone that are used as marker horizons. A 10-30m layer in the middle Waripi Limestone separates two thick sequences of peloid limestone/dolostone (Figure 2-2). The grains in this member are well sorted, angular to subangular, vary from 20-80% total content and average 0.3mm in size. A 50m (plus subordinate dolostone/limestone) member near the top of the Waripi Limestone is composed of 60-90% moderately sorted, angular to subangular quartz grains of 0.2mm average grainsize, increasing to 0.4-0.6mm at the base of the member. A third 5m-thick laminated sandstone member with well sorted, angular to sub-angular, 30-80% sand grains of 0.1mm average size, has been used to mark the upper contact of the Waripi Limestone (Figure 2-2, Plate 2-4e). In all cases the matrix is composed of micritic calcite or dolomite spar. Talc, tremolite and pyroxene are commonly present in the matrix of sandstones in both KLS1-1 and KLS3-1 and impart on what is normally grey sandstone a pasty white appearance (Plate 2-4b). A shale horizon approximately 5m thick was identified and sampled in KLS3-1 in the upper Waripi Limestone at the top of the upper sandstone layer (Figure 2-2). This layer was not identified in KLS1-1. Another shale layer was identified in drill hole KLS1-1 within the middle sandstone layers (Figure 2-2). A 60-80m horizon of limestone containing elongate to rounded foraminifera is present in the upper Waripi Limestone, bound top and bottom by sandstone (Figure 2-2). The foraminifera vary from 1-5mm in size, and constitute 50-80% of the rock (Plate 2-4d). Dolomite, anhydrite and native sulphur have replaced foraminifer grains in places where dolomitisation is prevalent in the matrix (Plate 2-8). These foraminifera are similar in size and shape to vughs in dolostone of the lower and middle Faumai Limestone that are usually infilled with dolomite quartz, anhydrite and native sulphur. Anhydrite nodules occur at three specific levels in the Waripi Limestone in KLS3-1, namely at the top between two sandstones, in the middle of the unit associated with sandstone and shale, and in a narrow band (~20m) near the base of the unit. They vary in shape from spherical to lenticular and are roughly elongate in direction of bedding (Plate 2-4c). Nodule size varies from <5mm to 50mm. The nodules at the base are the more spherical type.

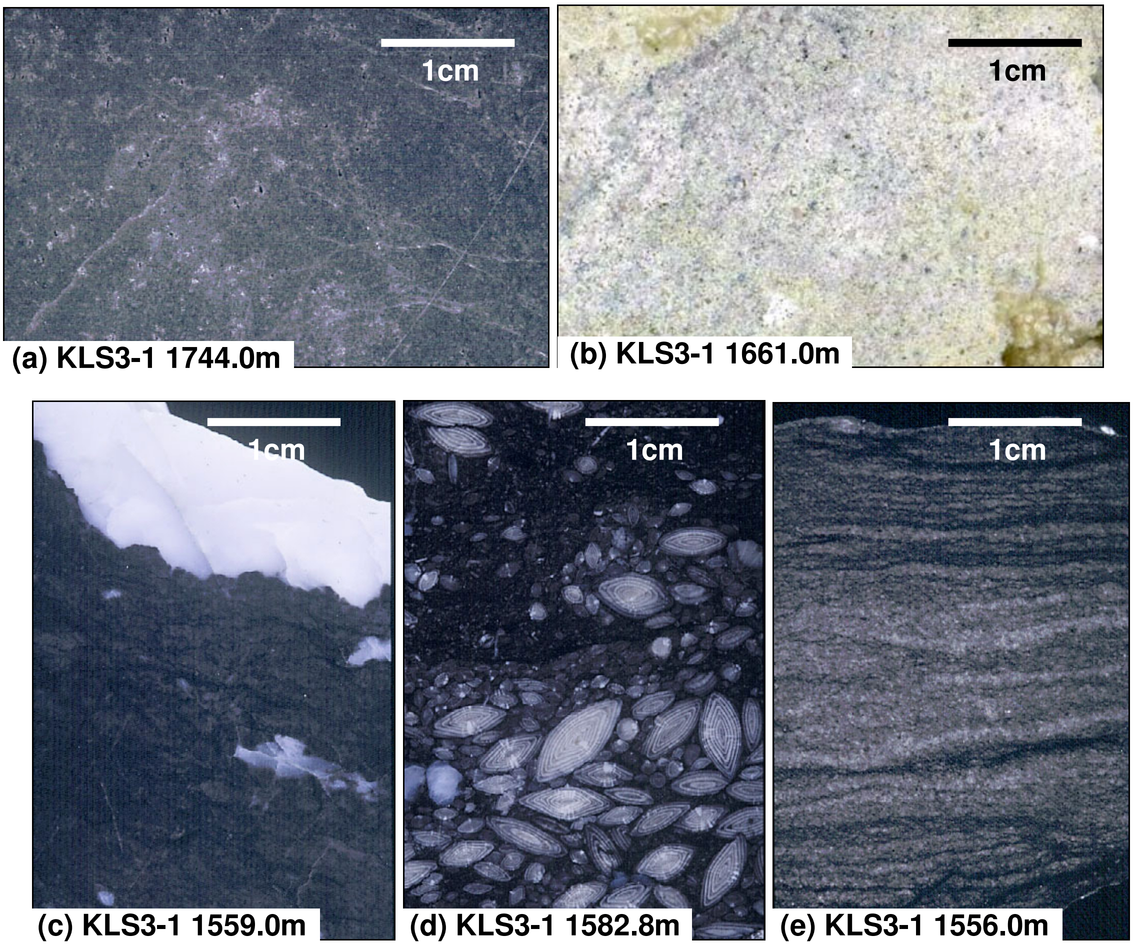

Plate 2-4 Examples of Waripi Limestone visible textures

(a) Medium grey peloid dolostone typical of the majority of the Waripi Limestone. The lines are fractures associated with lighter grey dolomite alteration. (b) Sandstone matrix that is normally dark grey is changed to white due to presence of amphibole-pyroxene-talc. (c) An anhydrite nodule from the upper Waripi Limestone oriented subparallel to sedimentary layering. (d) Foraminifera from the upper Waripi Limestone which resembles texture in the middle Faumai Limestone where leached holes have been infilled with coarse-grained carbonate. (e) Finely laminated sandstone that marks the upper contact of the Waripi Limestone.

New Guinea Limestone Group – Faumai Limestone (Tngf)

The Faumai Limestone is 350m thick in KLS3-1. The lower half of the Faumai Limestone is extensively dolomitised in both KLS1-1 & KLS3-1 and the only unaffected parts occur at the top of the unit (Figure 2-2). Identifiable Faumai Limestone in KLS1-1 and KLS3-1 consists of fossiliferous calcite limestone, dolomitised limestone and dolostone. Distinctive round foraminifer *lacazinella wichmanni* (Plate 2-5a and Plate 2-5c) dominate the uppermost limestones that are composed of uniform packstone, in which the foraminifer grains range from 1-2mm in diameter. A micritic calcite matrix supports the foraminifer grains that constitute up to 80% of the rock. This member is approximately 70m thick in KLS3-1. Below this in KLS1-1, there is another preserved limestone member containing a variety of carbonate grains. In this member the elongate foraminifer *lepidocyclina sp.* is common (Plate 2-5b). Also included in these upper layers are subordinate grains of echinoderms, bryozoa and coralline algae.

New Guinea Limestone Group – Sirga Sandstone (Tngs)

The thickness of the Sirga Sandstone intersected in drill hole KLS3-1 is approximately 20m. It unconformably overlies the Faumai Limestone and consists of a series of interbedded sandstones and fossiliferous carbonate rocks (Plate 2-6). The dominant carbonate is calcite, although dolomite is present in minor quantities. There are ~5m beds in the Sirga Sandstone with very high organic contents. The Kais-Sirga contact appears conformable, as a section at the top of the Sirga Sandstone contains 50% quartz grains and 50% foraminiferal grains of same species present in overlying limestone.

New Guinea Limestone Group – Kais Limestone (Tngk)

The original thickness of the Kais Limestone is not known as the top of the unit has an unconformable contact with Quaternary sediments. Only the lower part of the Kais Limestone has been examined in this study as upper sections do not host Kucing Liar mineralisation. The base is typified by limestone with packed elongate foraminifera up to 10mm long (Plate 2-7). These are dominantly *nummulite fichteli* plus minor amounts of *operculina* sp., and *operculinella*. Minor dolomite and scattered quartz grains are present in samples collected from the lower Kais Limestone.

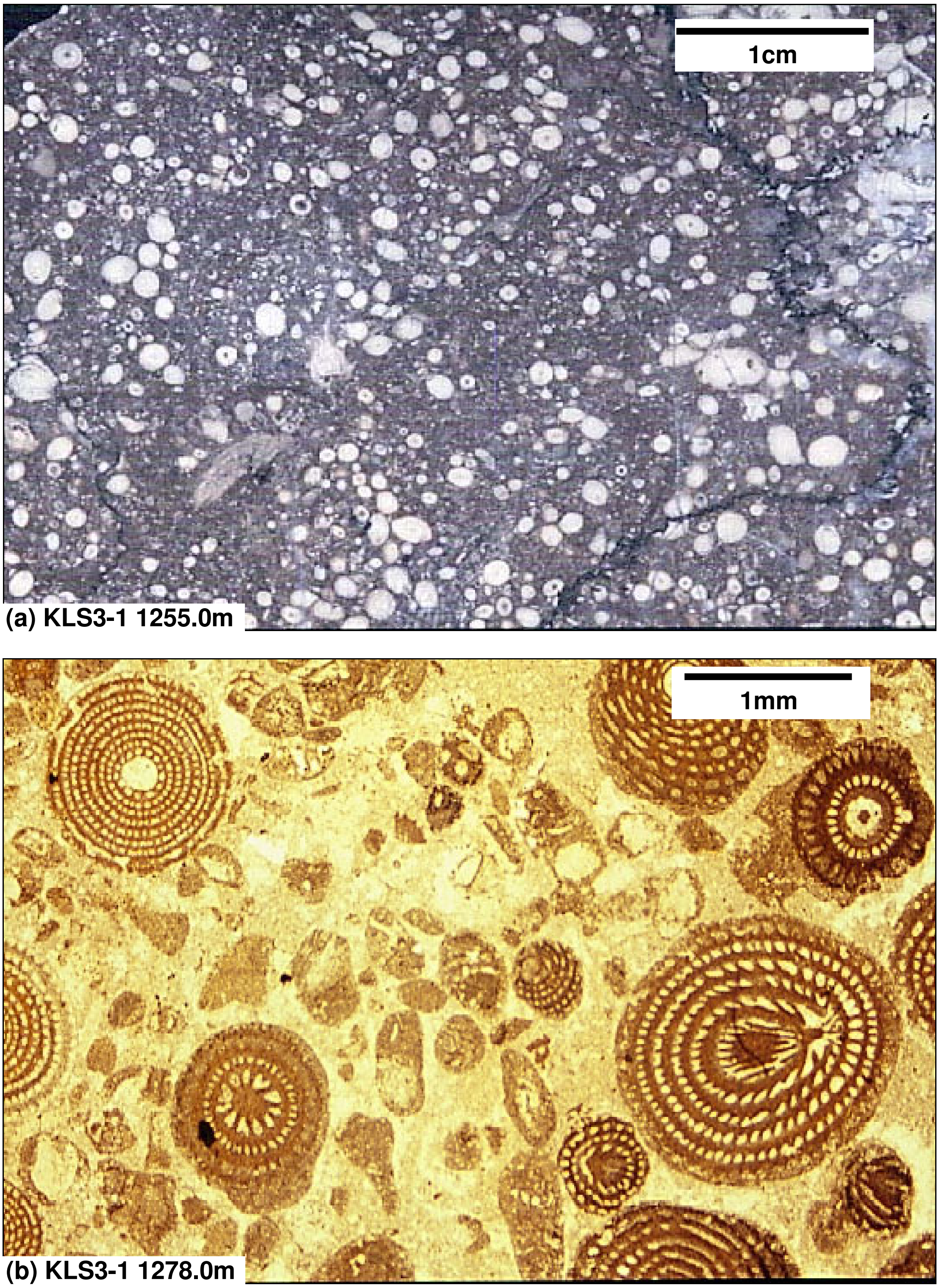

Plate 2-5 Examples of Faumai Limestone visible and micro-textures

(a) Distinctive round foraminifera (lacazinella wichmanni) *from the upper Faumai Limestone (b) Grains of* Lacazinella wichmanni *are calcite while the intervening matrix has been converted to dolomite. Plane light image of a stained section.*

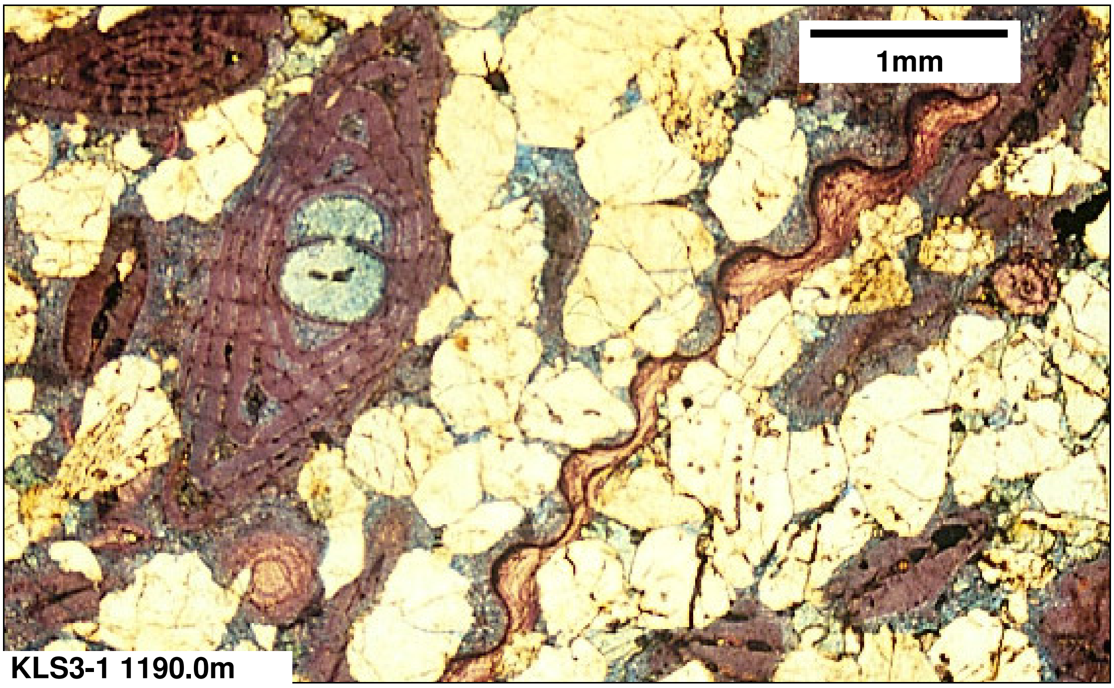

Plate 2-6 Example of Sirga Sandstone

Photomicrograph illustrating large nummulites fichteli *identical to those in the overlying Kais Limestone mixed with coarse sand grains*. P*ink and purple colours indicate calcite while blue indicates dolomite. Plane light image of a stained section.*

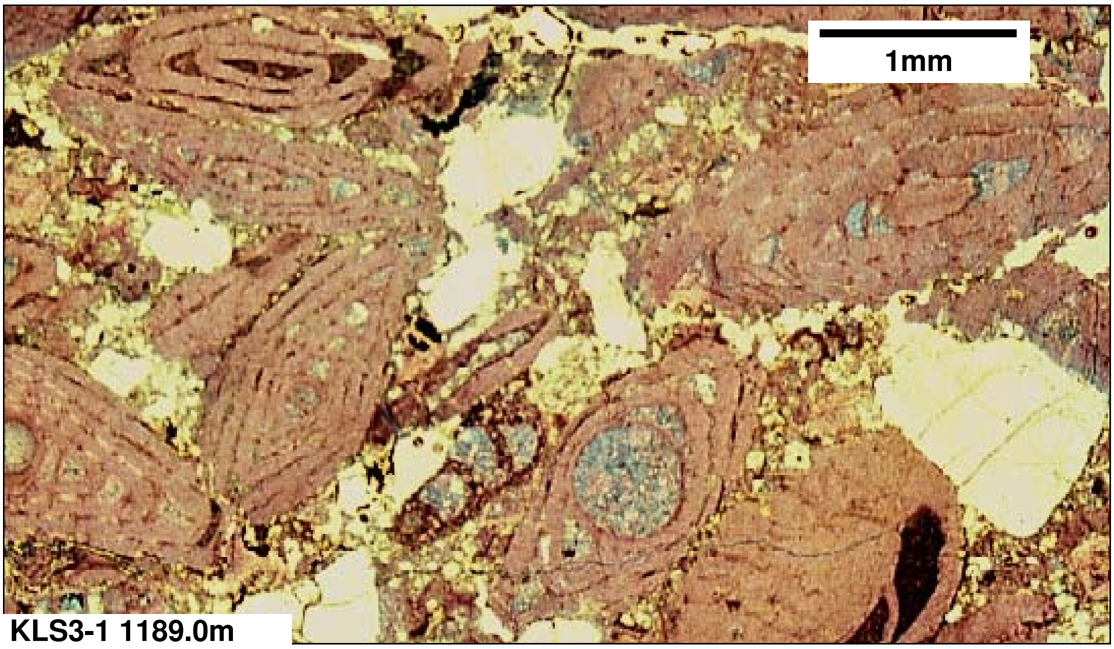

Plate 2-7 Example of Kais Limestone

Photomicrograph illustrating nummulites fichteli *that dominate the lower Kais Limestone. Much smaller spiral-shaped* operculina sp. *is also present. Foraminifera are (pink) calcite while some have ferroan dolomite (blue) in the centre. The matrix between grains has been altered to dolomite (yellowish). The large white grains are quartz. Plane light image of a stained section.*

2.2.2 Textures developed in low-intensity distal alteration

Dolomitisation

Samples from KLS1-1 and KLS3-1 indicate variable effects of dolomitisation (Plate 2-8) most common as well as calc-silicate alteration. The number of dolomitisation events and their extents are unknown, and their precise relationships to the mineralizing hydrothermal systems are also not clear. The effects of dolomitisation vary from minor alteration of grains and matrix resulting in the preservation of the original texture (Plate 2-9), to the complete replacement of original calcite by dolomite spar, resulting in the destruction of the original sedimentary texture. All textures between these two endmembers are represented. Complete replacement of calcite by dolomite occurs over very short distances as seen in composition columns for samples in KLS1-1 and KLS3-1 (Figure 2-2). The scale of replacement is less than the sample spacing of 10m as the change in carbonate is complete between two samples. Figure 2-2 also illustrates that calcite limestone is preserved near sandstone horizons at the top and bottom of the Faumai and Waripi Limestone units. A spatial association between texturally destructive dolomitisation and sandstone layers is apparent in KLS3-1. Contacts between unaltered limestone and texturally destructive dolostone range from gradational to sharp and a complete loss of sedimentary texture occurs over a 4m interval in KLS3-1 between 1278.8m and 1282.3m. Layers are discretely altered to equigranular dolomite sparite and are intercalated with dolostone where the original texture can be identified. Dolomitisation is most intensely developed in the limestone-only packages of these two units between sandstone horizons. Dolostone is grey in the Waripi Limestone (Plate 2-8a) and brownish-beige in the Faumai Limestone (Plate 2-8f). Spherical to elongate pores filled with anhydrite and dolomite (Plate 2-10) in the middle and lower parts of the Faumai Limestone are very similar in size, shape and abundance to similar features in foraminiferal limestone of the upper Waripi Limestone. The matrix in these rocks consists of subhedral to euhedral dolomite grains and the pores are filled to varying degrees with varying amounts of calcite, dolomite or native sulphur (Plate 2-8c, d & e).

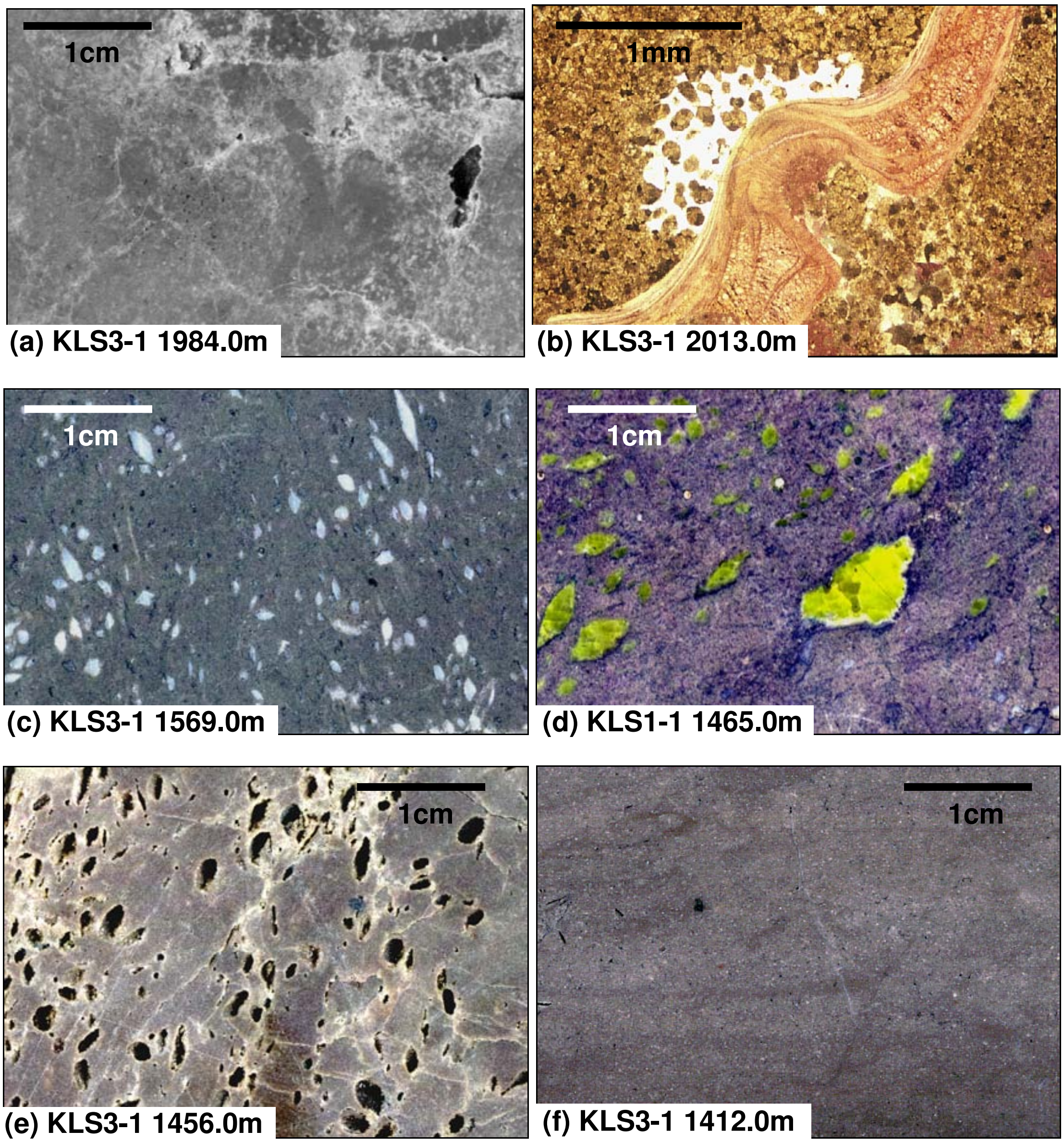

Plate 2-8 Examples of dolomitisation textures

(a) Fine-grained dolomitised peloid limestone such as is common in the Waripi Limestone. (b) An unidentified bioclast composed of original calcite is surrounded by a matrix of yellowish dolomite from the lower Waripi Limestone. The grey-white area in the view is a cavity. Plane light image of a stained section. (c) White anhydrite and dolomite infilling cavities that are shaped like foraminiferal grains from uppermost Waripi Limestone. (d) An example of the same limestone layer depicted in (c), though here the foraminifer-like voids are infilled with native sulphur (e) A sample from the lower Faumai Limestone believed to have been foraminiferal limestone where the fossil grains have been dissolved. The vughs are lined with quartz and/or dolomite. Note similarity with (c) above. (f) Intense dolomitisation results in complete destruction of clastic sedimentary textures in this dolomite sparite, although some semblance of the layering appears to be preserved as darker zones of dolomite in this sample from the middle Faumai Limestone.

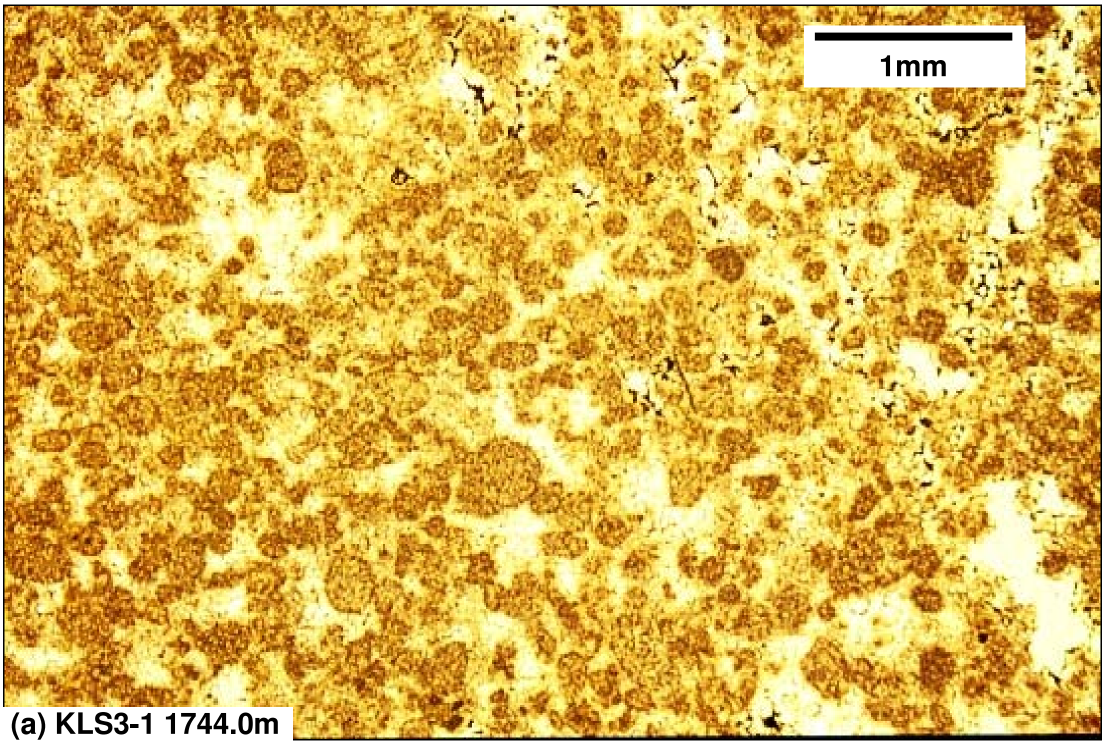

(a) KLS3-1 1744.0m

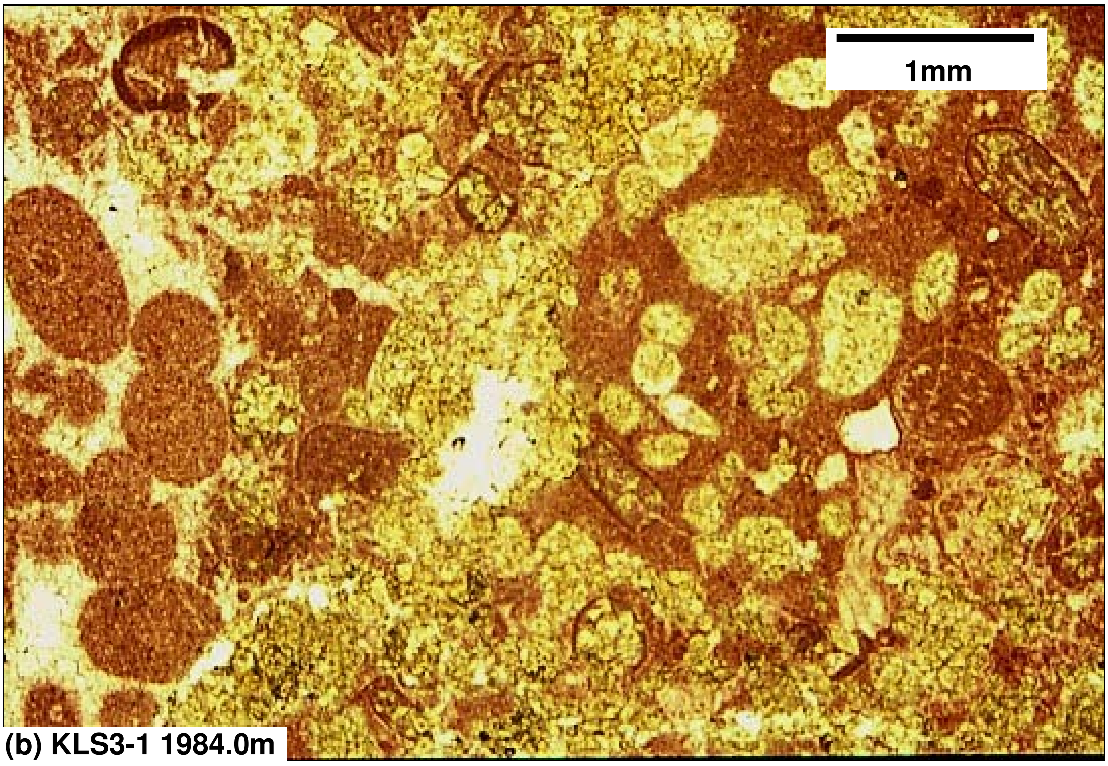

(b) KLS3-1 1984.0m

Plate 2-9 Examples of dolomitisation micro-textures in peloid limestone

(a) Yellowish dolomite surrounds reddish micritic calcite peloid grains and voids (white patches). Plane light image of a stained section (b) Micritic calcite peloid limestone replaced by two generations of dolomite. A yellowish-coloured type replaces the peloid grains at right and bottom, while a paler variety of dolomite preferentially affects matrix rather than the micritic grains and surrounds pores (white). Plane light image of a stained thin section.

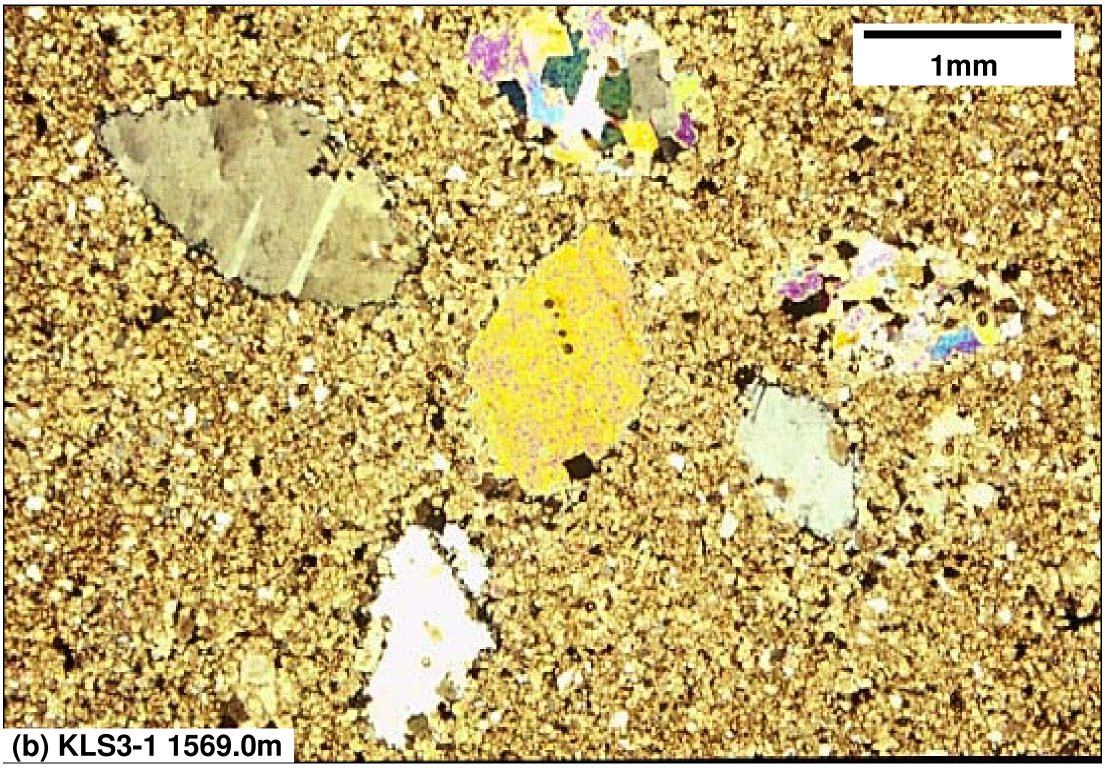

Plate 2-10 Examples of dolomitisation micro-textures in foraminiferal limestone

(a) Foraminifer grains composed of primary calcite surrounded by very fine-grained dolomite spar. Plane light image of a stained thin section. (b) Dolomite (high birefringence, twinned) and anhydrite (moderate birefringence, polycrystalline) infilling cavities that are of similar shape though much smaller than foraminifera illustrated in plate (a). Cross polarised light image of a stained thin section.

Distal silicate alteration

Distinctly hydrothermal alteration is also present in both KLS1-1 and KLS3-1 as represented by plagioclase, pyroxene, garnet, epidote, amphibole and talc. As with dolomitisation, this alteration is preserved as a continuum of textural and mineralogical changes that, while subtle, are identifiable in hand specimen samples. Changes were identified using comparison of rock samples from the same stratigraphic positions in different locations. These changes are described and illustrated in the following section with reference to rock sample photography. The variability of the characteristic compositions and sedimentary textures present within the host rock types (Plate 2-11a & d) are preserved despite hydrothermal alteration. In KLS1-1, the Ekmai Limestone has a very fine-grained glassy texture, coloured white and green, locally containing pods of coarser-grained red garnet, while the overlying Waripi Limestone has the same fine-grained grey dolomite appearance to that observed in KLS3-1. Petrographically this alteration appears as equigranular plagioclase interspersed with coarser grains of pyroxene. Clumps of epidote and garnet were also identified in alteration style. The upper Ekmai Limestone is characterised by isolated quartz grains whereas the middle Ekmai Limestone is devoid of quartz, providing distinction of position within the stratigraphic unit (Figure 2-2). The heterogeneous nature of the Ekmai Limestone is preserved in pyroxene-feldspar and garnet alteration (Plate 2-11a-c). Sandstone has a grainy texture, and although the Ekmai Sandstone is fine-grained it is easily distinguished from limestone or shale. Quartz grains commonly persist in intensely altered zones and grey sand grains are easy to recognise in a matrix of white to pale green pyroxene (Plate 2-11d-f). However, some samples of altered sandstone demonstrate that sand grains have been eroded during calc-silicate alteration (Plate 2-12).

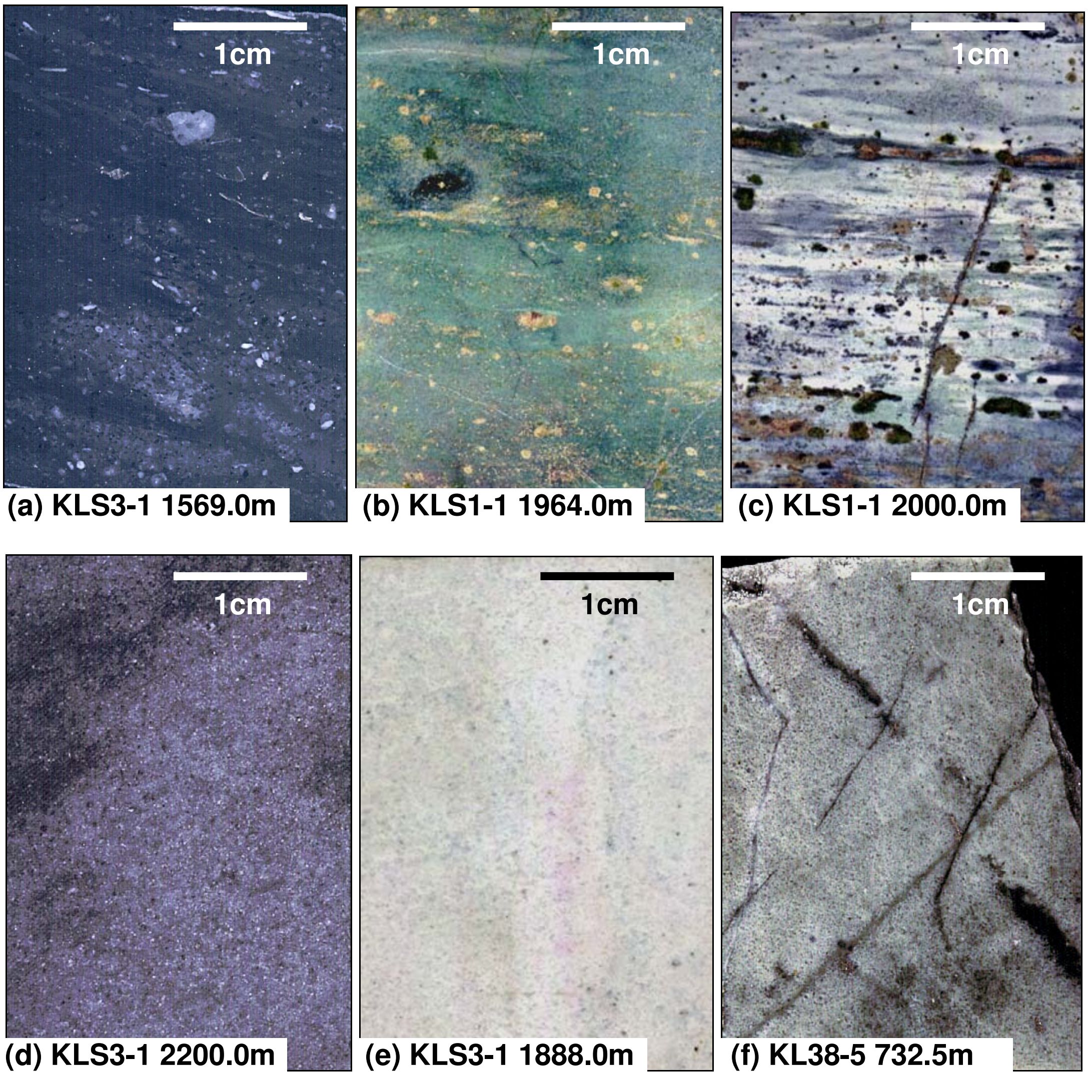

Plate 2-11 Examples of distal hydrothermal alteration

Photographs of samples taken from KLS1-1 and KLS3-1 demonstrating the effects of hydrothermal alteration. (a) Unaltered shale from the upper Ekmai Limestone illustrates the heterogeneous texture created by clusters of organic clasts and sand grains. (b) Green pyroxene and red garnet in altered shale from KLS1-1 displaying excellent preservation of original sedimentary texture as compared to (a). (c) Grey calcite-magnetite/white feldspar/red garnet altered Ekmai Limestone. (d) Unaltered sandstone with the organic material still visible as dark matrix near the top of the photograph. (e) A sample taken from KLS3-1 to illustrate calcite-talc-amphibole alteration of sandstone. (f) An example of clinopyroxene altered sandstone taken from the lowermost part of the mineralised zone in Kucing Liar.

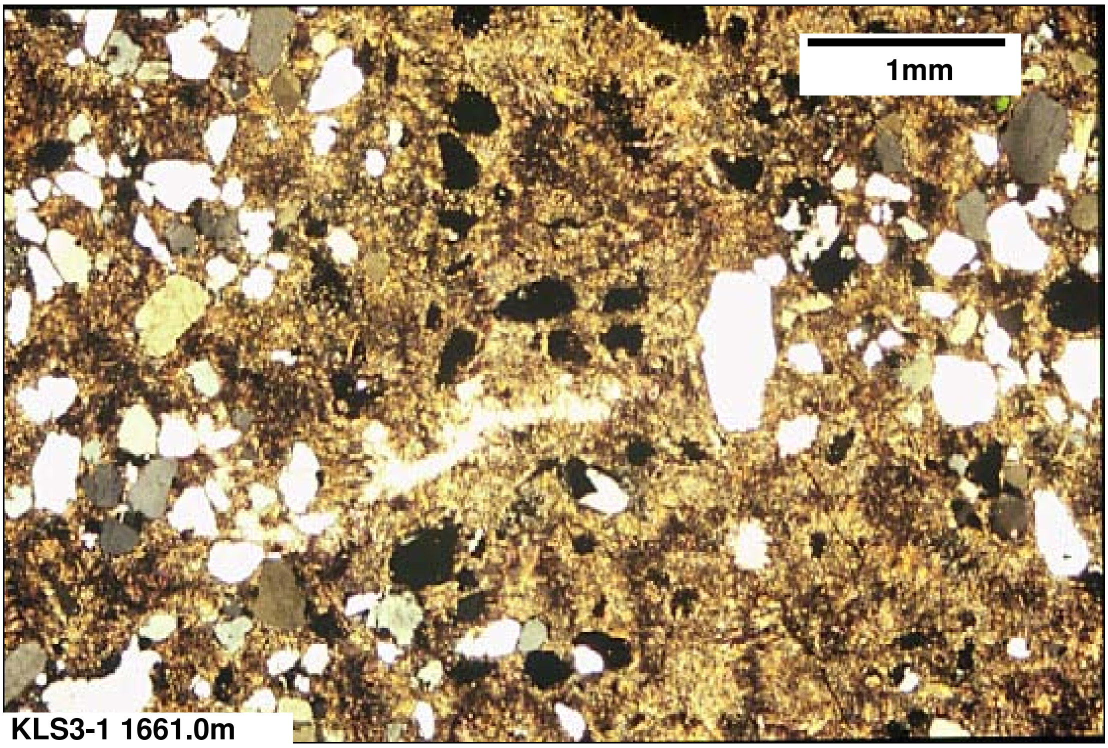

Plate 2-12 An axample of hydrothermal micro-textures in sandstone

A photomicrograph of altered sandstone illustrates the progression of hydrothermal alteration. Dissolution of quartz grains (black holes) is associated with replacement of the matrix by amphibole and talc (yellow-brown). Crossed polarised light.